

Switchable aqueous catalytic systems for organic transformations

Nikita Das ¹ & Chandan Maity ¹✉

In living organisms, enzyme catalysis takes place in aqueous media with extraordinary spatiotemporal control and precision. The mechanistic knowledge of enzyme catalysis and related approaches of creating a suitable microenvironment for efficient chemical transformations have been an important source of inspiration for the design of biomimetic artificial catalysts. However, in “nature-like” environments, it has proven difficult for artificial catalysts to promote effective chemical transformations. Besides, control over reaction rate and selectivity are important for smart application purposes. These can be achieved via incorporation of stimuli-responsive features into the structure of smart catalytic systems. Here, we summarize such catalytic systems whose activity can be switched ‘on’ or ‘off’ by the application of stimuli in aqueous environments. We describe the switchable catalytic systems capable of performing organic transformations with classification in accordance to the stimulating agent. Switchable catalytic activity in aqueous environments provides new possibilities for the development of smart materials for biomedicine and chemical biology. Moreover, engineering of aqueous catalytic systems can be expected to grow in the coming years with a further broadening of its application to diverse fields.

The enzymes in natural biosynthetic processes work in aqueous environment, where they reach amazing levels of efficiency, and selectivity. Enzyme catalysis is often used in nature to control formation of molecules and/or complex structures for achieving homeostasis, motility, and signaling processes. The catalytic processes generally take place in parallel, and the required spatiotemporal control of the catalytic activity often entails its modulation by physicochemical stimuli such as small molecules, light, temperature, and pH¹. Stimuli-induced enzyme catalysis and the underlying mechanism have been an important source of inspiration for the design of biomimetic artificial catalysts. Scientists have devoted many efforts to obtain artificial catalytic systems in aqueous environment with the aim of mimicking the levels of performance of natural enzymes^{2,3}. However, the artificial catalysis usually takes place according to the initially chosen reaction conditions, and lacks the control over the chemical process⁴. The rate of chemical transformations can be modulated employing stimuli-triggered catalysts having stimuli-responsive features in the structure of the catalytic systems^{5–8}.

In aqueous media, the artificial switchable catalysis could be a key factor to develop more efficient nature-inspired catalytic systems for the green industrial processes^{9,10}. At this regards, organic transformations have been studied in water as the reaction medium^{11–14}. Water possesses many desirable characteristics as reaction medium due to its environmental friendliness, high polarity, large cohesive energy, high heat capacity, and hydrogen bonding abilities that may influence reaction rate and selectivity^{12,15}. Besides, use of water as reaction medium benefits chemical processes by allowing mild reaction conditions, simplifying operations, and sometimes providing unforeseen reactivities and selectivities^{13,16}. Despite this, organocatalytic reactions in aqueous environments encounter considerable challenges such as poor reactant solubility,

¹Department of Chemistry, School of Advanced Sciences (SAS), Vellore Institute of Technology (VIT), Vellore 632014 Tamil Nadu, India. ✉email: chandan.maity@vit.ac.in

transition states destabilization due to disturbance of hydrogen bonding interactions, and poor hydrolytic stability of catalytic intermediates or chemical species^{17,18}. Over the past few decades, attempts have been made to overcome these challenges for various organic transformations in aqueous media^{14,19–22}. However, achieving reversible control over chemical transformations in aqueous environment remains a challenge.

There have been few studies devoted to the controlled organic transformations in aqueous environment employing switchable catalytic systems, whose catalytic activity can be switched ‘on’ and ‘off’ by stimuli. These systems are promising candidates for the application in biological environments and/or industrial processes. Generally, these catalyst systems have smart structural features that respond reversibly according to the presence/absence of stimuli for speeding up or slowing down the reaction rate. The switching mechanism of these systems mostly depends on (i) accessibility of the active sites of catalytic system that can be modified by the stimulus due to change in electronic, steric, or cooperative effects in the systems, and (ii) availability of suitable microenvironment via aggregation/dissociation of the catalytic system in presence/absence of external stimulus. For example, temperature-, pH-responsive catalytic systems usually change the aggregation state for suitable microenvironment in presence/absence of stimuli, whereas light-, small molecule-responsive catalytic systems depend on the electronic, steric, or cooperative effect of the system for accessing the active site of the catalyst.

In this review, we describe stimuli-induced artificial switchable catalytic systems with classification in accordance to the stimulating agent (Fig. 1). The scope of this review encompasses organic reactions in aqueous buffer solution or water/organic solvents mixture. We discuss the state-of-the-art and identify the challenges in this field. We describe “in water”¹⁴ stimuli-switchable systems, where the reactants, catalyst, and products are present in aqueous (buffer) solution. We also describe “on water”²⁰ stimuli-switchable systems, which comprise emulsions, hydrogels, and supramolecular assemblies or immobilized catalyst on solid support, where water exerts a critical effect on the reaction rate. However, biocatalysis^{23–25} for organic reactions in aqueous medium have not discussed here as they involve enzyme engineering, and are not fully synthetic systems. Altogether, switchable catalysis for organic transformations in “nature like” environment would find applications in smart materials such as

self-healing materials, controlled delivery, spatiotemporal on-demand drug synthesis, therapeutics, and soft robotics. The examples of different chemical transformations have summarized in Table 1, and this article is divided according to the stimulating agent employed for switchable catalytic systems, which we now describe.

pH-induced switchable catalytic systems

Change in pH in aqueous solution can substantially change the property of the medium and physicochemical responses of the species that present in the solution. In nature, many enzymatic reactions are pH-sensitive^{26–29}. pH stimulus can regulate the catalytic activity of natural enzymes, where the conversion of substrate to product takes place within the microenvironment of a catalytic site. As an example, triosephosphate isomerase (TIM) is a crucial enzyme in the glycolytic pathway, which catalyzes the reversible isomerization of D-glyceraldehyde 3-phosphate to dihydroxyacetone phosphate. The forward and reverse reactions catalyzed by TIM is pH dependent³⁰. At the active site of TIM, proton transfer from dihydroxyacetone phosphate to glyceraldehyde phosphate is carried out by the carboxylate side-chain of Glu165/167³¹ and by the imidazole side-chain of His95³².

In comparison to natural enzymes, it is difficult to replicate the complex enzymatic environment for artificial systems. Incorporation of pH-responsive features in artificial supramolecular systems, pH-triggered catalytic activity can be realized^{33–38}. However, pH-induced switching of catalytic activity due to aggregation/dissociation of supramolecular systems remains relatively unexplored. In an example, Zhang et al.³⁹ reported pH-switchable artificial hydrolase activity, where a catalytic histidine residue was introduced at the edge of a pH-responsive peptide, VK2H (Fig. 2a). By changing pH from acidic to alkaline, the peptide exhibited a conformational transition from random coil to β -sheet. The β -sheet self-assembled to long fibrils, where histidine residues extended in an ordered array as an effective catalytic microenvironment. The fibrils showed significant esterase activity by catalyzing the hydrolysis of *p*-nitrophenyl acetate (pNPA) (kinetic efficiency = $19.18 \text{ s}^{-1} \text{ M}^{-1}$) in tris-HCl buffer (Table 1, Entry 1). The role of histidine as catalytic site was confirmed by replacing histidine residue of the peptide with glycine (VK2G), which self-assembled into fibrils, but with much

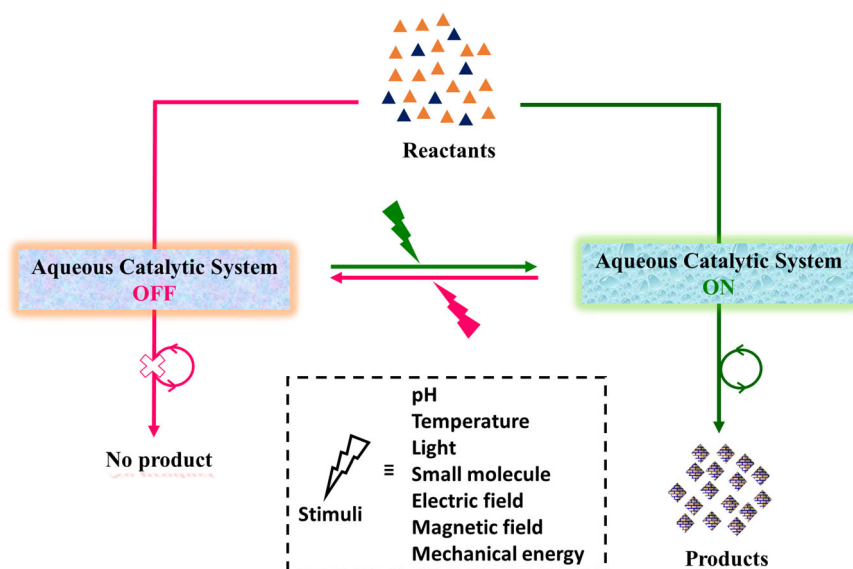


Fig. 1 Switchable aqueous catalytic system. A schematic representation of switchable catalytic systems in aqueous environments. Presence or absence of trigger can module the catalytic activity in switch ‘on’/‘off’ mode for organic reactions.

Table 1 The summary of switchable catalytic systems for chemical transformations in aqueous environments.

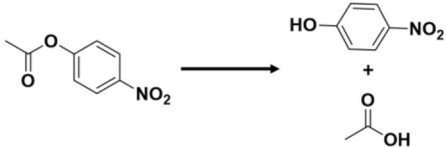
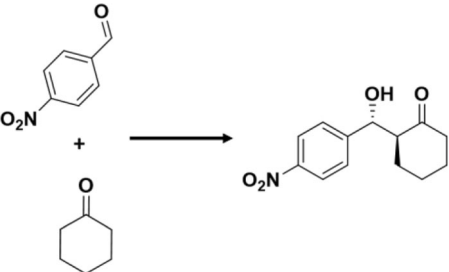
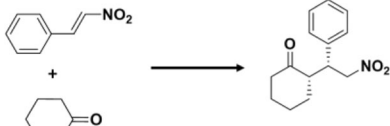
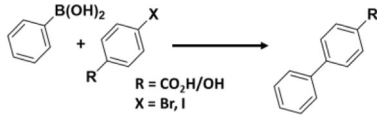
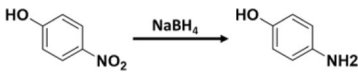
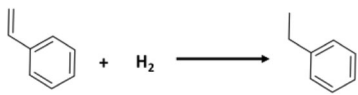
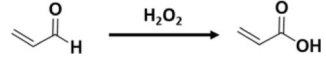
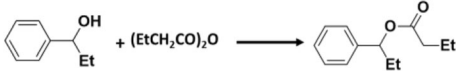
Entry no.	Chemical transformations	Catalyst moiety, Medium ^{Reference}	Stimuli	Catalysis status, Yield
1	Ester hydrolysis	Histidine, Tris-HCl buffer ³⁹	pH = 9.0	ON, .N.R.
2		Imidazole, Water ⁷³	pH = 6.0	OFF, .N.R.
3		Cavity of β-CD, Tris buffer (pH 8.7) ¹¹³	T > 32 °C	ON, .N.R.
4		Imidazole, PBS buffer (pH 7.2) ¹¹⁵	T < 32 °C	OFF, .N.R.
5		histidine, PBS buffer (pH 7.4) ¹¹⁷	UV light	ON, .N.R.
6		Imidazole-Zn complex, PBS buffer (pH = 7.6) ¹²²	Visible light	OFF, .N.R.
7		Isoindoline, Water ⁴⁰	UV light	ON, .N.R.
8	Aldol reaction		Visible light	OFF, .N.R.
9		L-proline, Water ⁵⁰	pH > 4.5	ON, 99%
10		L-proline, Water ⁵¹	pH < 5	OFF, 0%
11		L-proline, Water ⁷²	pH = 4.0	ON, 81% (ee)
12		L-prolineamide, Water ⁷⁴	pH = 7.0	OFF, 2% (ee)
13		L-proline, Water ⁸⁰	pH = 7.0	ON, 89% (ee)
14		L-proline, Water ¹³⁴	pH = 4.0	OFF, 37% (ee)
15		L-proline, Water ¹⁷⁶	T = 50 °C	ON, 95%
16	Michael reaction	Isoindoline, Water/THF ⁴⁰	T = 25 °C	OFF, 53%
17			T = 40 °C	ON, 83%
18			T = 25 °C	OFF, 10%
19			T = 30 °C	ON, 96% (ee)
20			T = 80 °C	OFF, 12% (ee)
21			CO ₂ (5 Mpa)	ON, 99%
22			No CO ₂	OFF, 0%
23			T = 50 °C	ON, 94%
24			T = 25 °C	OFF, 79%
25			pH = 6.7	ON, 23%
26			pH = 3.6	OFF, 0%
27	Suzuki reaction	Pd-NP, Water ⁵⁶	pH > 7.0	ON, >94%
28			pH < 7.0	OFF, No reaction
29	Reduction of nitrophenol	Au-NP, Water ⁵⁷	pH = 5.0	ON, .N.R.
30		PBT, Water ¹⁷³	pH = 9.2	OFF, .N.R.
31			CO ₂ & light, N ₂	ON, 96%
32	Hydrogenation of styrene	Pd-NP, Water/toluene ⁶²		OFF, 0%
33		Pd, Water ¹²⁸	pH = 3.0-4.0	ON, 99%
34			pH = 7.0-8.0	OFF, 0%
35			Visible light	ON, >99%
36			UV light	OFF, 0%
37	Acrolein oxidation	Active Se, Water/dioxane ⁷⁶	T = 50 °C	ON, >90%
38			T = 20 °C	OFF, No reaction.
39	Acetylation	DMAP, Water ⁸¹	T = 5 °C	ON, 98%
40			T = 50 °C	OFF, No reaction

Table 1 (continued)

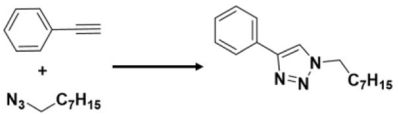
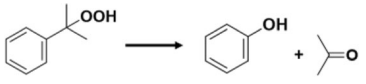
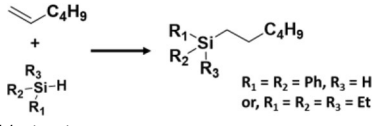
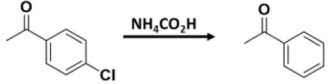
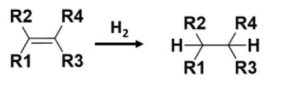
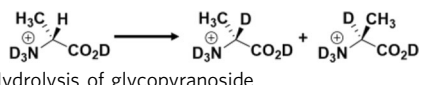
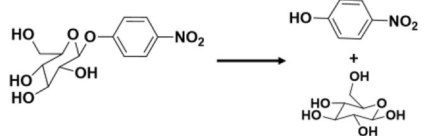
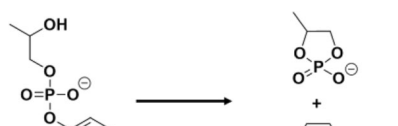
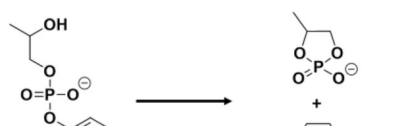
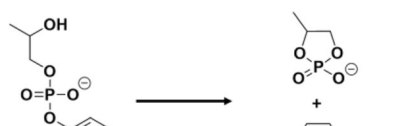
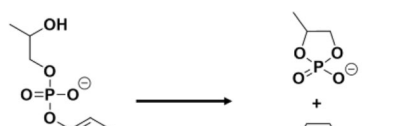
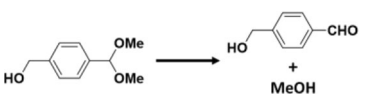
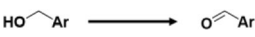
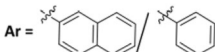
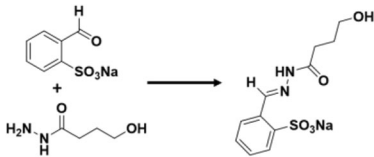
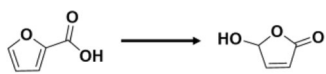
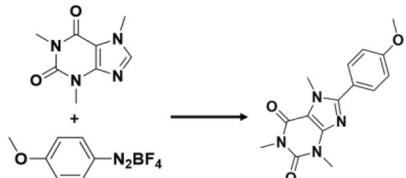
Entry no.	Chemical transformations	Catalyst moiety, Medium ^{Reference}	Stimuli	Catalysis status, Yield
24	Click reaction 	Cu(PPh ₃) ₂ NO ₃ , Water/organic reagent bilayer ⁸²	T < 32 °C T > 32 °C	ON, ^{-.N.R} OFF, No reaction
25	Decomposition of hydroperoxide 	Ph ₃ CPF ₆ , Water/organic reagent bilayer ⁸²	T < 32 °C T > 32 °C	ON, ^{-.N.R} OFF, No reaction
26	Hydrosilylation 	H ₂ PtCl ₆ , Water/organic reagent ⁸²	T < 32 °C T > 32 °C	ON, ^{-.N.R} OFF, No reaction
27	Dechlorination 	Pd-NP, Water/toluene ⁹⁷	T < 32 °C, T > 32 °C,	ON, 99% OFF, No reaction
28	Hydrogenation of alkene 	Ru-NP, Water ¹⁰⁵	T > 39 °C T < 39 °C	ON, ^{-.N.R} OFF, No reaction
29	Racemization 	Aldehyde and pyridinium group, D ₂ O/ CD ₃ CO ₂ D ¹¹²	UV light (λ = 365 nm) Visible light (λ > 490 nm)	ON, 95% OFF, 3%
30	Hydrolysis of glycopyranoside 	Biscarboxylic acid, Water ¹¹⁹	UV light (λ = 365 nm) Visible light	ON, ^{-.N.R.} OFF, ^{-.N.R.}
31	Transphosphorylation 	Zn(II)-based catalyst, HEPES buffer (pH 7.0) ¹²³	Visible light UV light (λ = 365 nm)	ON, ^{-.N.R.} OFF, ^{-.N.R.}
32		Zn(II)-based catalyst, HEPES buffer (pH 7.0) ¹²⁴	UV light (λ = 365 nm) Visible light (λ = 465 nm)	ON, ^{-.N.R.} OFF, ^{-.N.R.}
33		Zn(II)-based catalyst, Pseudo-aqueous solution ¹⁴⁰	Presence of CO & Cl ⁻ Absence of CO and Cl ⁻	ON, 100% OFF, No reaction
34		Cu(II)-based catalyst, HEPES buffer (pH 7.0) ¹⁷⁰	Oxidative potential Reductive potential	ON, ^{-.N.R.} OFF, ^{-.N.R.}
35	Hydrolysis of acetal 	Acid catalysis in 'nanoflask', Water-saturated toluene ¹²⁷	UV light (λ = 365 nm) Visible light	ON, ^{-.85%} OFF, ^{-.55%}

Table 1 (continued)

Entry no.	Chemical transformations	Catalyst moiety, Medium ^{Reference}	Stimuli	Catalysis status, Yield
36	Oxidation 	Cu(I)-bpy & TEMPO, Aqueous borate buffer (pH 9.5)/acetonitrile (1/1) ¹⁴³	ssDNA antitrigger sequence ssDNA trigger sequence	ON, ^{-N.R} OFF, No reaction
37		Aneli system, Water/organic substance ¹⁷⁷	No CO ₂ CO ₂ & magnetic field	ON, >94% OFF, No reaction
38	Hydrazone formation 	Aniline, PBS buffer (pH 7.5) ¹⁶⁵	Glycine betaine methyl ester Ester hydrolysis	ON, ^{-N.R} OFF, ^{-N.R}
39	Oxidation of furoic acid 	PBT, Water ¹⁷³	CO ₂ & light N ₂	ON, >99% OFF, No reaction
40	Arylation 	PBT, Water ¹⁷³	CO ₂ & light, N ₂	ON, 85% OFF, No reaction

^T temperature, ^{-N.R} not reported, ^{CD} cyclodextrin, ^{PBS} phosphate-buffered saline, ^{HEPES} 4-(2-hydroxyethyl)-1-piperazineethanesulfonic acid, ^{Tris} tris(hydroxymethyl)aminomethane, ^{IEP} isoelectric point, ^{ILS} ionic liquid surfactant, ^{TACN} 1,4,7-triaza-cyclononane, ^{TEMPO} 2,2,6,6-tetramethylpiperidine-1-oxyl, ^{NP} nanoparticle, ^{PBT} Poly(bisthiophene).

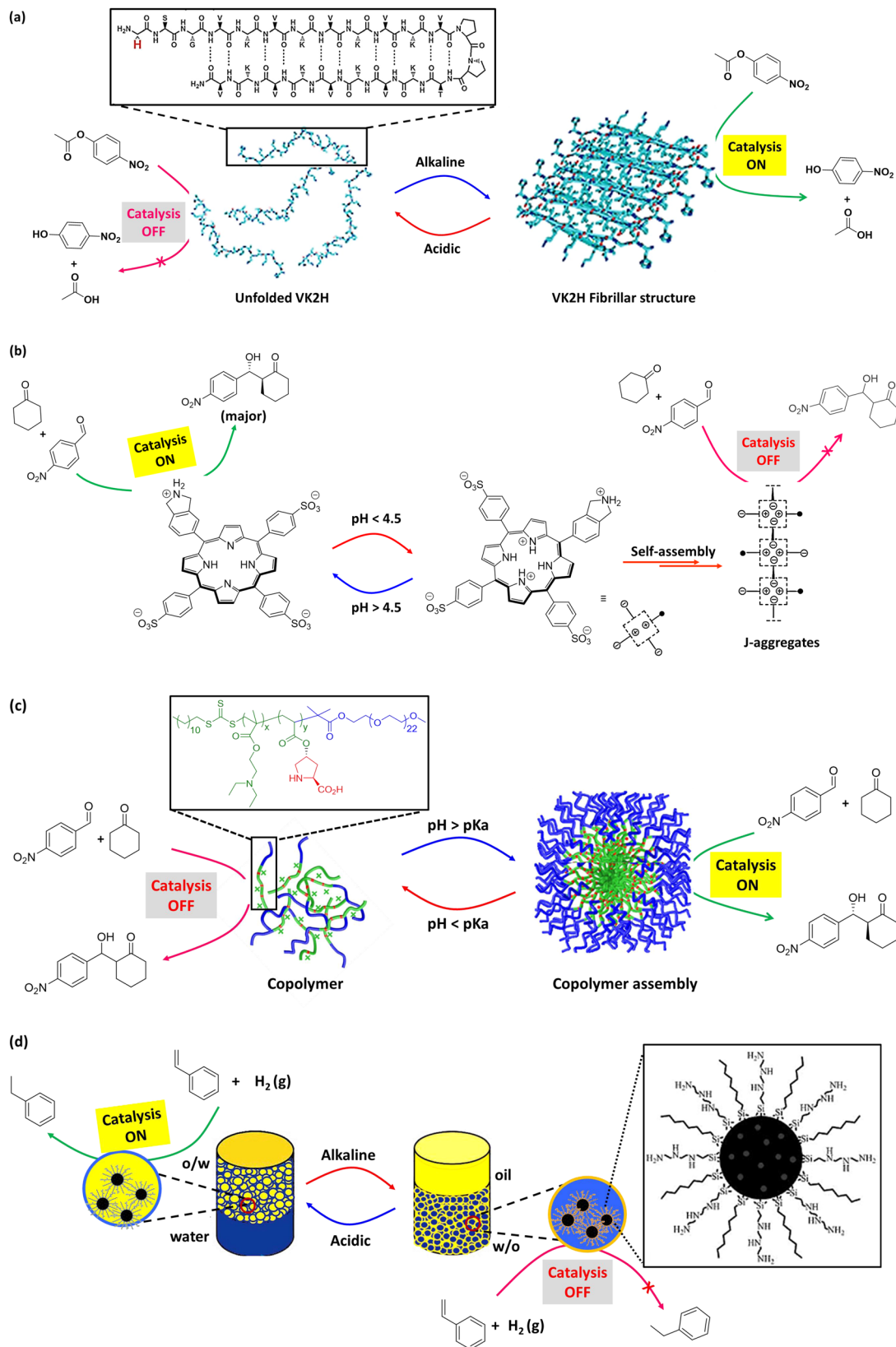
reduced catalytic activity. Besides, the peptide formed a hydrogel at higher concentrations, which is also catalytically active. In the self-assembled form, the histidine residues were exposed on the edges of the fibril, which provided the active site for substrate binding. Switchable catalytic activity was realized by pH-induced disassembly of the fibrils into random coils. Changing the pH between acidic (pH 6.0) and basic (pH 9.0), the phase behavior can be reversibly realized from gel to fluid, where the un-assembled random coils were catalytically inactive.

Employing amphiphilic molecule, pH-Induced modulation of catalytic activity of a supramolecular system was demonstrated by Arlegui et al.⁴⁰ (Fig. 2b). In this example, supramolecular system showed catalytically inactivity in aggregated state of the amphiphile, whereas catalytic activity was realized at dissociated state. The catalytic activity of cyclic secondary amine was demonstrated in an amphiphilic meso-(4-sulfonatophenyl)porphyrin derivative by adjusting the homogeneity of the aqueous solutions via pH change. In neutral aqueous solutions, the highly soluble free-base form of the porphyrin derivative showed enamine-based organocatalysis. In contrast, the porphyrin core was protonated under acidic conditions, and led to the formation of self-assembled structures. The protonation of the central pyrrolic core at acidic pH (typically below pH 4.8) induced the formation of J-aggregates, which was stabilized by ion-pair contacts between the cationic porphyrin centers and the peripheral anionic sulfonate groups. As a result, porphyrin-based pyrrolidine derivatives flocculate and the catalytic activity is fully suppressed. There is no aldol product formation even after 8 days at acidic pH (pH = 3.6) (Table 1, Entry 8). In comparison, the catalysis of the aldol reaction between cyclohexanone and p-nitrobenzaldehyde (pNB)

took place by isoindoline moiety with excellent yield (99%) and selectivity (93:7 anti:syn mixture of the aldol products) in the solution of higher pH value (pH = 6.7). However, at acidic pH, the catalyst aggregates can be easily separated from the reaction products via centrifugation. Thereafter, neutralization and desalting could provide the sulfonated amine-porphyrin hybrids, which retains their catalytic activity, and can be reused. Though, there is a substantial decrease of catalytic activity after few cycles.

Besides aldol reaction, isoindoline-functionalized amphiphilic porphyrin derivative was employed for Michael reaction between cyclohexanone and 2-nitrostyrene. However, poor yield (23%) of Michael adduct was reported even after three days in the solution of higher pH value, whereas no conversion was reported at lower pH value (Table 1, Entry 16). Nevertheless, the aggregation state of amphiphilic porphyrin derivatives and their catalytic activity can be controlled by means of pH stimulus. It is worth noting that self-assembled state of supramolecular systems can switch catalysis 'on' or 'off' depending on availability of suitable active-site microenvironment for the reactant(s) and favorable effect of the system to access the active-site for catalysis. For example, cooperative effect favors pNPA hydrolysis³⁹ in self-assembled state of V2K2H, whereas self-assembled state of amphiphilic porphyrin derivative⁴⁰ flocculates and therefore substrates of aldol reaction cannot access the catalytic sites, resulting switching 'off' the catalysis.

Polymeric materials, in response to pH stimuli, can undergo structural and/or property change, such as surface activity, chain conformation, solubility⁴¹. Immobilization of organocatalyst moiety within such polymer scaffolds may result in formation of aggregates with desired microenvironment, where efficient and



selective organic reactions could be possible⁴². In this regard, proline is used as one of the popular organocatalyst that facilitate chemical transformations similar to type 1 aldolase enzyme catalysis^{43,44}. Proline-catalyzed aldol product can be formed in the hydrophobic microenvironment through an enamine

mechanism, where water content at the catalytic site has an impact on the selectivity of the final product. Higher reaction rates and improved (stereo)selectivity could be obtained in the presence of small amount of water, whereas high water concentration can significantly lower the conversions and

Fig. 2 pH-switchable catalytic systems. **a** Schematic representation of the pH-switchable VK2H peptide as artificial hydrolase. The peptide showed conformational transition from unfolded random coil to β -sheet via changing the pH from acidic to alkaline. (Inset: chemical structure of peptide VK2H). The fibril structure can catalyze the hydrolysis of pNPA, whereas the unfolded structure is catalytically inactive. Switching the catalytic activity can be controlled by altering the pH. Adopted with permission from ref. 39, copyright 2017 Wiley-VCH Verlag GmbH & Co. KGaA, Weinheim. **b** pH-switchable organocatalysis with amine-porphyrin hybrid in aqueous solution. Formation of J-aggregates, at acidic pH, suppressed the catalytic activity of Isoindoline moiety of the hybrid, whereas deaggregated state of the hybrid at higher pH resulted efficient aldol reaction. Adopted with permission from ref. 40, copyright 2020 WILEY-VCH Verlag GmbH & Co. KGaA, Weinheim. **c** A schematic of assembly behavior of polymer structure in aqueous solution at different pH (inset: the structure of the polymer), and aggregation-induced aldol reaction that catalyzed by proline moiety. Adopted with permission from ref. 51, copyright 2020 Elsevier B.V. **d** Schematic of pH-induced emulsion inversion for styrene hydrogenation. At acidic pH, the catalyst can efficiently convert the substrate to product, whereas the reaction is terminated at basic pH (inset: The structural description of silica microsphere with catalytically active center). Adopted with permission from ref. 62, copyright 2013 WILEY-VCH Verlag GmbH & Co. KGaA, Weinheim.

selectivities^{19,45}. Moreover, proline functionalized with nonpolar moieties demonstrated the importance of hydrophobic environment for proline-catalyzed aldol reaction^{46,47}. Proline can be anchored to polymer scaffolds for asymmetric aldol reactions with a range of ketones and aldehydes in aqueous environment^{48,49}. In one example, Prado et al.⁵⁰ employed an amphoteric alternating copolymers of hydrophobic phenylmaleimide and hydrophilic vinylpyrrolidone for supporting L-proline-catalyzed aldol reaction in aqueous buffer solution (Table 1, Entry 9). It is reported that near the isoelectric point (IEP) of the polymer (around pH 4), an aggregated form of the polymer scaffold favored the formation of high enantioselective product (91% yield, 81% ee). This high enantioselectivity is attributed to the exclusion of water from the polymer aggregates, resulting stabilization of the transition state. In contrast, the hydrophilicity of the aggregates increased at higher pH (pH 7). The asymmetric aldol reaction could be observed (with 99% yield), but reduced the enantioselectivity (2% ee). This is attributed to presence of high water concentration at the active center that influenced the transition state. Thus, control over the polymer aggregates and aggregation-induced selectivity of aldol product could be realized in response to pH change in aqueous environment. Likewise, Tang et al.⁵¹ reported L-proline-functionalized pH-responsive block copolymer for asymmetric aldol reaction in water. In this study, a series of block copolymers were employed having L-proline as catalyst moiety, poly(-diethylaminoethylmethacrylate) (PDEA) as pH-responsive segment, and methyl polyethylene glycol (mPEG) as hydrophilic moiety (Fig. 2c). Catalytic activity and stereoselectivity of these copolymer catalysts were examined for asymmetric aldol reaction between pNB and cyclohexanone at different pH values (pH = 4.0, pH = 7.0) (Table 1, Entry 10). The result indicated that catalytic activity and stereoselectivity can be affected by the pH value of aqueous solution and the structures of copolymer catalyst assemblies. At acidic pH (pH = 4.0), PDEA fragment of copolymers became hydrophilic due to protonation of amine group and displayed smaller hydrodynamic sizes (~20 nm), poor yield (26%), and selectivity (37% ee). At pH 7.0 (close to the pKa value), copolymer self-assembled to hydrophobic PDEA core and hydrophilic mPEG corona. At this pH (pH 7.0), suitable ratio of hydrophilic to hydrophobic segment of the aggregate effectively attracted substrates to the catalytic sites and avoided large amount of water near the catalytic active center, which can disturb the transition state⁵². The catalytic activity and selectivity of aldol product (75% yield and 89% ee) were increased. However, larger hydrodynamic size (~220 nm) at basic pH (pH = 9.0) indicated the deprotonation of the amine groups leading to more hydrophobic PDEA blocks and less yield of aldol product (59%). Therefore, modulation in chemical conversion and selectivity can be observed by adjusting suitable ratio of hydrophilic to hydrophobic segment of a polymeric material by varying pH.

Besides assemblies in polymeric or supramolecular systems, heterogeneous catalysts have been used for organic transformations due

to their site-specific selectivity, minimized metal trace in reaction medium, recyclability, and ease in product separation^{53,54}. Among them, core-shell microstructures with inorganic cores and organic shells have been employed for controlled catalysis in aqueous environments⁵⁵. For example, Zhang et al.⁵⁶ employed pH-responsive core-shell microstructures for Suzuki reaction in aqueous media. In this example, Pd nanoparticles (Pd-NPs) were embedded in the shell layer of polystyrene-co-poly[2-methacrylic acid 3-bis(carboxymethylamino)-2-hydroxypropyl ester] (PS-co-PGMA-IDA). The fabricated structures were stable in basic aqueous solution (pH > 7), and can activate aryl boronic acid to form biaryl product with aryl halides at room temperature (Table 1, Entry 17). High yield of biaryls (>85%) was achieved for hydrophilic substrates, however, poor yield (<30%) was obtained for hydrophobic substrates. Moreover, at lower pH, the core-shell structure was destabilized via protonation of the methacrylate part of the copolymer. This resulted in decrease in reaction rate by restricting access to the Pd particles. Thus, employing Pd-NP fabricated PS-co-PGMA-IDA, the Suzuki reaction in aqueous environment could be switched 'on' and 'off' by adjusting the pH of the medium. In this way, accessibility of suitable confined environment for an organic reaction can be controlled by changing pH of the solution. Likewise, core-shell microstructures involving Au-NPs for switchable catalysis was demonstrated by Xiao et al.⁵⁷, where Au-NPs were enveloped by an interpenetrating gel network of methylenebisacrylamide and polyvinylpyrrolidone (PVP) (Table 1, Entry 18). At higher pH (pH > 6), shrinkage of the gel structures occurred due to deprotonation of —COOH group of methacrylate, resulting reduced hydrogen bonding and drainage of water molecules from the core. As a consequence, it closed the diffusion gateways for the reactants for catalytic reduction of 4-nitrophenol with the help of NaBH₄ (rate of reaction, $K = 1.0 \times 10^{-1} \text{ min}^{-1}$ at pH 9.2). In comparison, PVP developed hydrogen bonding with methacrylate groups at lower pH, which permitted the reactants to come in close proximity of the Au-centers, resulting successful reduction reaction (rate of reaction, $K = 6.1 \times 10^{-1} \text{ min}^{-1}$ at pH 5.0). Thus, pH-responsive NP-based catalytic systems can be created by combining organic ligands and metal-based NPs⁵⁸.

Catalytic system with Pickering emulsion (PE) provides a distinct platform, which can perform more than traditional catalysis technology⁵⁹. Generally, PE, composed of aqueous-organic biphasic system stabilized by solid particles, can compartmentalize droplets to control the chemical process in response to stimulus, as well as the isolation or protection of incompatible reagents and the sensitive species that can be easily affected by the harsh reaction conditions^{60,61}. PE-based systems with control over wettability and interfacial tension of emulsions can provide switchable PE-based catalysts (*vide infra*). pH-responsive PE-based catalytic systems utilize sub-micrometer-sized particles having functional groups that can protonate/deprotonate upon pH change, resulting pH-regulated wettability of the systems. In an example, Yang et al.⁶² reported an in situ preparation method of sub-micrometer size solid catalysts for hydrogenation of

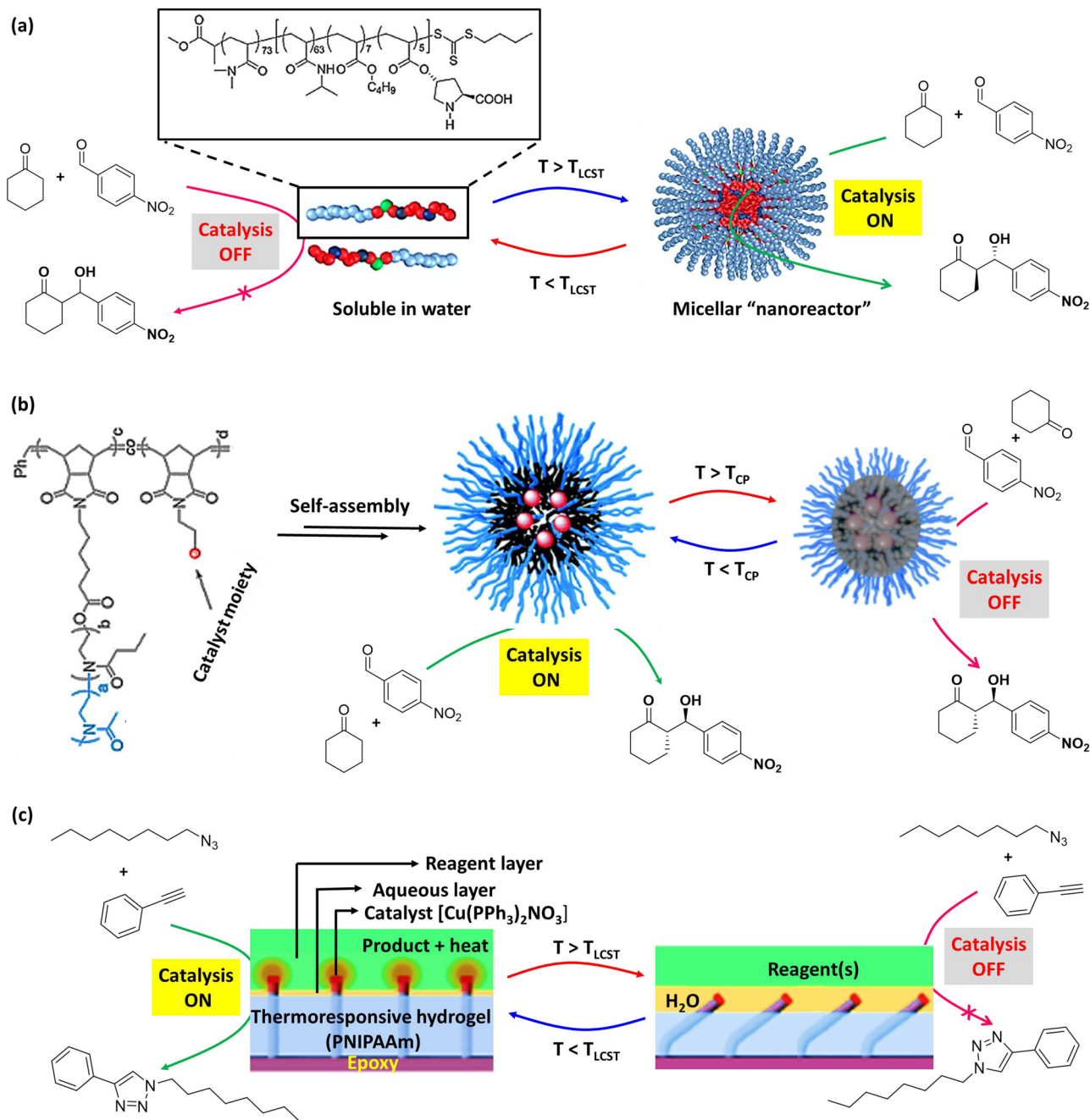


Fig. 3 Thermoresponsive polymer-based switchable catalytic systems. **a** Positive thermoresponsive micellar nanoreactor—at lower temperature, the polymer is soluble in water and Aldol reaction is ‘off’ due to the absence of suitable environment (Inset: chemical structure of the polymer). At elevated temperature, micelle is formed and provided suitable environment for L-proline-catalyzed Aldol reaction. Adopted with permission from ref. ⁷², copyright 2013 American Chemical Society. **b** Negative thermoresponsive micellar nanoreactor—at lower temperature, formation of micelle allowed the substrates to access catalyst, whereas at higher temperature polymer chain collapsed to hydrophobic globules, which inhibit the formation of intermediate, resulting poor selectivity. Adopted with permission from ref. ⁸⁰, copyright 2021 American Chemical Society. **c** Self-regulating thermoresponsive catalyst surface—structure tips are coated with catalyst and upright/bent tips corresponding to ‘on/off’ catalysis. Below LCST of PNIPAAm, the catalyst tips enter the reagent layer, resulting an exothermic click reaction. Above the LCST, the PNIPAAm contracts and the structures bend, removing the catalyst from the reagent layer and turning ‘off’ the reaction. Adopted with permission from ref. ⁸², 2012, Nature Publishing Group, a division of Macmillan Publishers Limited.

styrene via tuning the pH value of solution (Fig. 2d). In this example, hairy silica microspheres were fabricated with a mixture of hydrophilic, pH-sensitive $(\text{MeO})_3\text{SiC}_3\text{H}_6(\text{NHC}_2\text{H}_4)_2\text{NH}_2$ and relatively hydrophobic $(\text{MeO})_3\text{Si}(\text{CH}_2)_7\text{CH}_3$ via covalent linkage. Pd-NPs were deposited onto these hairy silica microspheres. This

way, interfacially active and pH-responsive solid catalyst was formulated in an organic (toluene)/aqueous biphasic system. The protonation and deprotonation via pH change make the catalyst surface hydrophilic/hydrophobic, resulting switchable emulsion. The system formed an oil-in-water (o/w) emulsion at low pH

(pH 3.0 to pH 4.0) due to protonation of triamine-functional group on the surface. In these o/w emulsion, hydrophobic styrene moieties clustered inside the oil droplets. The system availed the favorable conditions for hydrogenation reaction of styrene to ethylbenzene (99% yield) due to the location of the catalyst particles at the interface of the emulsion droplets (Table 1, Entry 20). In contrary, the system is converted to a water-in-oil (w/o) emulsion by increasing the pH value (pH 7.0 to 8.0), where triamine-functional group deprotonated and become hydrophobic. As a result, Pd-NPs of the silica microsphere cannot be accessed by the substrate as it prefers the oil phase, and therefore, the reaction was terminated. The surface of these particles, this way, can be switched between hydrophilic/hydrophobic via protonation or deprotonation by pH change. Moreover, the catalysts can be recycled many times without significant loss of activity. Likewise, pH-switchable catalytic microreactors based on PE were also reported for the reduction of *p*-nitroanisole with NaBH_4 ^{63,64}.

Temperature-induced switchable catalytic systems

Temperature is an important stimulus for enzyme catalysis as the rate of enzyme catalytic reactions depends on temperature⁶⁵. Reactions, catalyzed by enzymes, generally stop at higher temperature due to enzyme denaturation. Temperature-responsive artificial switchable catalyst systems have been developed mostly based on temperature-responsive polymers fastened to a catalytic active segment. The temperature-responsive behavior is observed when the temperature is fluctuated around lower critical solution temperature (LCST) of a polymer^{66–69}. Depending on the hydrophobic and hydrophilic nature of polymer chain above or below of LCST, the catalytic activity of these polymer materials can be switched ‘on’ and ‘off’ by obtaining a suitable micro-environment for chemical reactions via adjustment in temperature (*vide infra*). Moreover, employing such polymers as a carrier for metal nanoparticles, nanoreactors have been achieved with the control over catalytic activity just by changing temperature. With respect to temperature-responsiveness, these nanoreactors are broadly classified into two categories—(a) positive temperature-responsive nanoreactors, which deswell at lower temperature, and (b) negative temperature-responsive nanoreactors, which deswell at higher temperature.

Positive thermoresponsive nanoreactors are generally designed in such a way that they show the catalytic activity at elevated temperature. Polymeric micelles have been employed as positive thermoresponsive nanoreactors because of their distinct core-shell structure with confined hydrophobic core domain^{70,71}. In an example, Zayas et al.⁷² reported a temperature-induced switchable micellar nanoreactor for asymmetric aldol reaction in water. In the nanoreactor, L-proline was attached with a block copolymer having a permanently hydrophilic block [poly(dimethylacrylamide), PDMA], and a thermoresponsive block [poly(N-isopropylacrylamide) (PNIPAm)] (Fig. 3a). Above the LCST (ranging from 25 to 40 °C) of the polymer, the PNIPAm block became hydrophobic that resulted in micelles of ~15–20 nm in diameter, where the L-proline moiety located within the hydrophobic PNIPAm core. In this way, L-proline moieties in the nanoreactor obtain an ideal hydrophobic environment for catalysis (Table 1, Entry 11). The reactions were efficient at high temperature (50 °C) with excellent yields (95%) and enantioselectivity (96% ee). In contrast, lowering the temperature (below the LCST of the polymer) resulted disassembly of the nanoreactors to water-soluble polymers, and reduction in aldol product formation (53% yield at 25 °C). However, the aldol product was precipitated in ice bath and could be isolated by centrifugation. The aqueous solution of polymer could be reused for next catalytic cycle via reformation of the nanoreactors by increasing the

temperature above LCST. Likewise, nanoreactors have been realized via immobilizing different organocatalysts, such as imidazole⁷³ for hydrolysis of pNPA (Table 1, Entry 2), L-prolineamide⁷⁴ for aldol reaction (Table 1, Entry 12) with thermoresponsive polymers in water.

Catalytic system with microgel can offer an attractive platform as microgels are porous particles consisting of a cross-linked polymeric network, and can form colloidal-stable dispersions in water⁷⁵. By changing temperature, substrates could diffuse through the porous network during swelling in water and can access the catalyst embedded in the network, whereas the molecules would be trapped inside the microstructure during deswelling. Thus, modulation in catalysis can be achieved via temperature-induced swelling/deswelling of microgels. In an example, Tan et al.⁷⁶ reported a temperature-responsive selenium-modified poly(N-vinylcaprolactam) microgel as glutathione peroxidase (GPx) mimic. Diselenide bonds inside the microgel was converted to seleninic acid through oxidation by H_2O_2 and used as colloidal catalyst for acrolein oxidation to acrylic acid (Table 1, Entry 22). The catalysis was ‘on’ (yield > 91%) at higher temperature (50 °C), whereas at lower temperature (20 °C) the catalysis was ‘off’ and microgel can be removed from the product. However, a substantial decrease in the yield of acrylic acid was reported in consecutive cycles, which is ascribed to higher viscosity of the reaction mixture leading to the deterioration of the diffusion process.

Negative temperature-responsive nanoreactors consisting PNIPAm fragment are often homogeneous below the LCST and can act as an efficient catalyst, whereas above LCST, they form globules, and become a heterogeneous system which shows poor catalytic activity^{77–79}. For example, Kuepfert et al.⁸⁰ demonstrated proline-functionalized negative thermoresponsive nanoreactor for aldol reaction in water with efficient catalysis and enantioselectivity (Fig. 3b). In this example, nanoreactors were prepared from proline-functionalized 2-oxazoline-based bottlebrush copolymers, in which the length of 2-oxazoline portion could be adjusted for tunable catalytic activities. Attachment of the proline along the bottlebrush copolymers created a hydrophobic core having the catalyst moiety and a thermoresponsive shell. Upon self-assembly of these bottlebrush copolymers in an aqueous solution, micellar nanoreactor system was generated that catalyze the asymmetric aldol reaction. The micellar nanoreactors exhibit tunable catalytic activity as a function of temperature. The modulation in hydrophobic behavior of the bottlebrush polymer affects the diffusion of substrate molecules to the core. At lower temperature (below the cloud point, T_{cp}), proline fragment of the polymer can catalyze the aldol reaction between pNB and cyclohexanone (Table 1, Entry 13) with good conversions (up to 97%) and stereoselectivities (up to 96% ee). In contrary, poor selectivity of the aldol product (12% ee at 80 °C) was obtained at higher temperature. It is proposed that the polymer chain collapse from hydrophilic coils to hydrophobic globules at higher temperature (above T_{cp}) resulting enhancement of water diffusion to the catalytic sites that inhibit the formation of stabilized transition state. However, at intermediate temperatures, higher stereoselectivity of the aldol product was observed, which indicated the dependency of water diffusion to the catalytic sites of the micellar nanoreactor is a function of temperature, and selectivity of the aldol product could be modulated via changing temperature. Likewise, thermoresponsive nanoreactor has been realized via immobilizing 4-(dimethylamino) pyridine (DMAP)⁸¹ for acylation reaction in water (Table 1, Entry 23).

Employing a negative-thermoresponsive hydrogel-based material, He et al.⁸² reported a seminal study about temperature-responsive ‘on/off’ switch for organic reactions. In this example, catalyst moiety was engineered to the tips of an epoxy

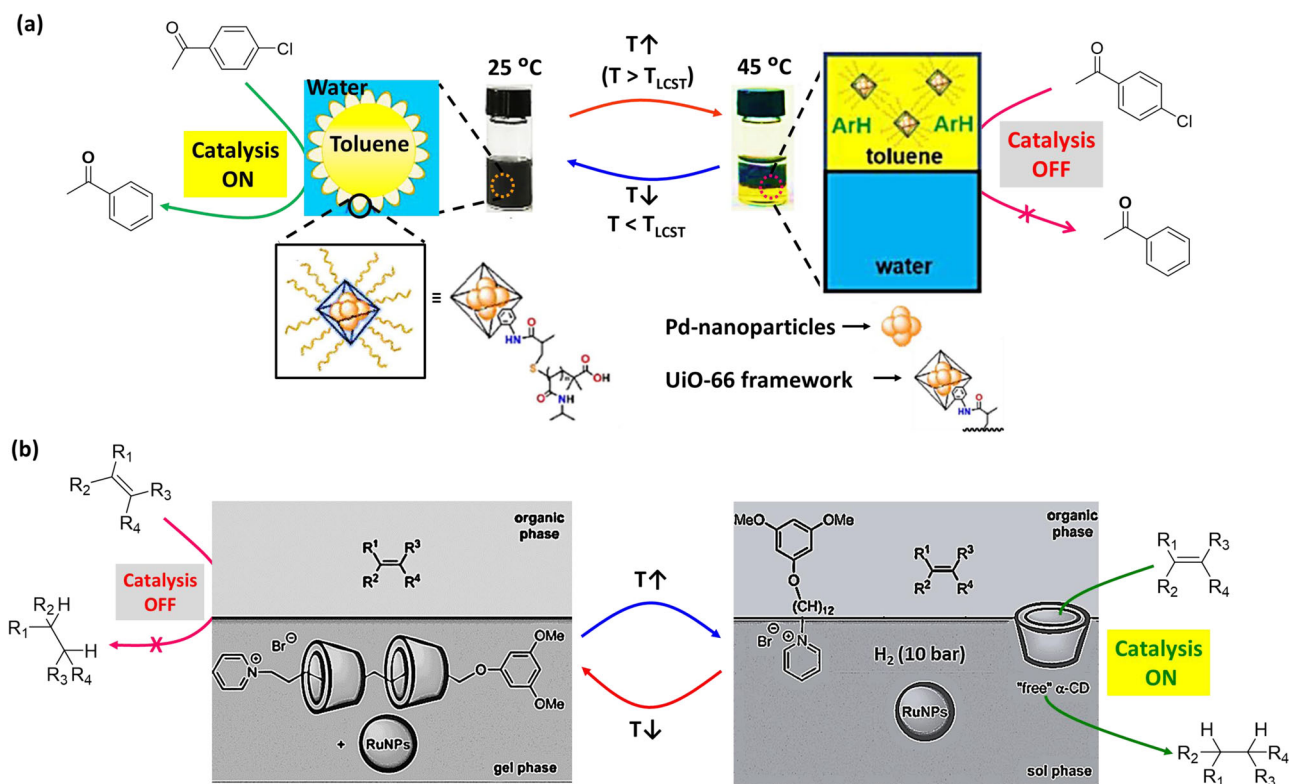


Fig. 4 Temperature-switchable nanoparticle-based catalytic systems. **a** PE-based catalytic system—Schematic for MOF-stabilized PE for dehalogenation reactions of chlorobenzene derivatives at 25 °C (Inset: structure of Pd-nanoparticle encapsulated thermoresponsive MOF). By increasing temperature, the system de-emulsified with phase separation and catalytic activity is switched 'off'. Adopted with permission from ref. ⁹⁷, copyright Royal Society of Chemistry. **b** Ru-NPs-based catalytic system—Ru-NPs embedded in the rotaxane-based gel phase, where the alkene cannot access the nanoparticle for catalytic transformation. When temperature has increased, the gel-sol transition occurred, and α -CD could play the role of mass transfer and bring alkenes into Ru-NPs-containing aqueous phase for their conversion into the corresponding alkanes. Adapted from ref. ¹⁰⁵, copyright 2012 WILEY-VCH Verlag GmbH & Co. KGaA, Weinheim.

microstructure via either physical adsorption or chemical covalent attachment process. The resulting assembled system was embedded within temperature-responsive hydrogel PNIPAm, which shows negative temperature-responsive behavior. The system was immersed in a liquid bilayer of aqueous/organic substance (reagent layer) (Fig. 3c). Employing this design, *click* reaction between octylazide and phenylacetylene was performed (Table 1, Entry 24). Below the LCST (32 °C, LCST of PNIPAm), the polymer was in its swollen state and the catalyst-functionalized tips could be found intruding into the reagent layer (octylazide and phenylacetylene). Therefore, the reagents can access $\text{Cu}(\text{PPh}_3)_2\text{NO}_3$ catalyst, which is on the tip of the microstructure, for *click* reaction. As it is an exothermic reaction, the temperature of the system increased, resulting contraction of the hydrogel above the LCST via expelling water molecules. Thus, the catalyst-bearing microstructure tips were removed from the reagent layer and catalysis was 'off' until the temperature changed to the LCST. Accordingly, self-regulated oscillation of catalysis was generated influencing on the LCST of the hydrogel. Besides the *click* reaction, Ph_3CPF_6 catalyzed decomposition of cumene hydroperoxide (Table 1, Entry 25), H_2PtCl_6 catalyzed hydrosilylation reaction between 1-hexene and triethylsilane/diphenylsilane (Table 1, Entry 26) have been successfully performed. By changing the reagent concentration (for controlling the rate of heat generation), the amount of liquid interface, or the microstructure geometry, the temperature oscillations and thereby the catalysis could be finely tuned. These materials are very similar to the living organisms in the sense that they could respond to the changes in their local environment through interconversions of

chemical and/or mechanical energy and self-regulating feedback loops⁸³.

Besides temperature-responsiveness, the morphology of the PNIPAm segment of a nanostructure has an impact on the activity of the catalyst, which is generally embedded within the hydrophobic core of the nanostructures. In a study, Lu et al.⁸⁴ reported a core-shell (CS) and core-shell-corona (CSC) type nanogels based on L-proline-functionalized hydrophobic core within a thermoresponsive PNIPAm shell. CS nanostructure consists a hydrophobic cross-linked core and a temperature-responsive cross-linked shell, while the CSC morphology consists an additional layer where the polymer chains are less cross-linked. Catalytic dependency of the nanostructures on temperature was examined at three temperatures—at 4 °C where PNIPAm is hydrophilic and solvated, at 25 °C where PNIPAm is somewhat hydrophobic, and at 40 °C (above the LCST of PNIPAm) where it is fully hydrophobic and in a collapsed state. For an asymmetric aldol reaction between pNB and cyclohexanone, it was found that the catalytic activity was enhanced with increasing temperature for CS nanogel structures (40% conversion, 86% ee at 4 °C; 88% conversion, 96% ee at 40 °C), whereas a drop in activity was observed at elevated temperatures with CSC nanostructures (66% conversion, 95% ee at 4 °C; 28% conversion, 97% ee at 40 °C). In comparison, the CSC nanogel showed greater catalytic activity than CS nanogel at low temperature (4 °C), which is attributed to the lower-crosslinking density of the CSC nanostructure, resembling the micellar-type morphology and catalytic activity. With increasing temperature of CS nanogel, the collapse of PNIPAm segment resulted in increase of hydrophobic

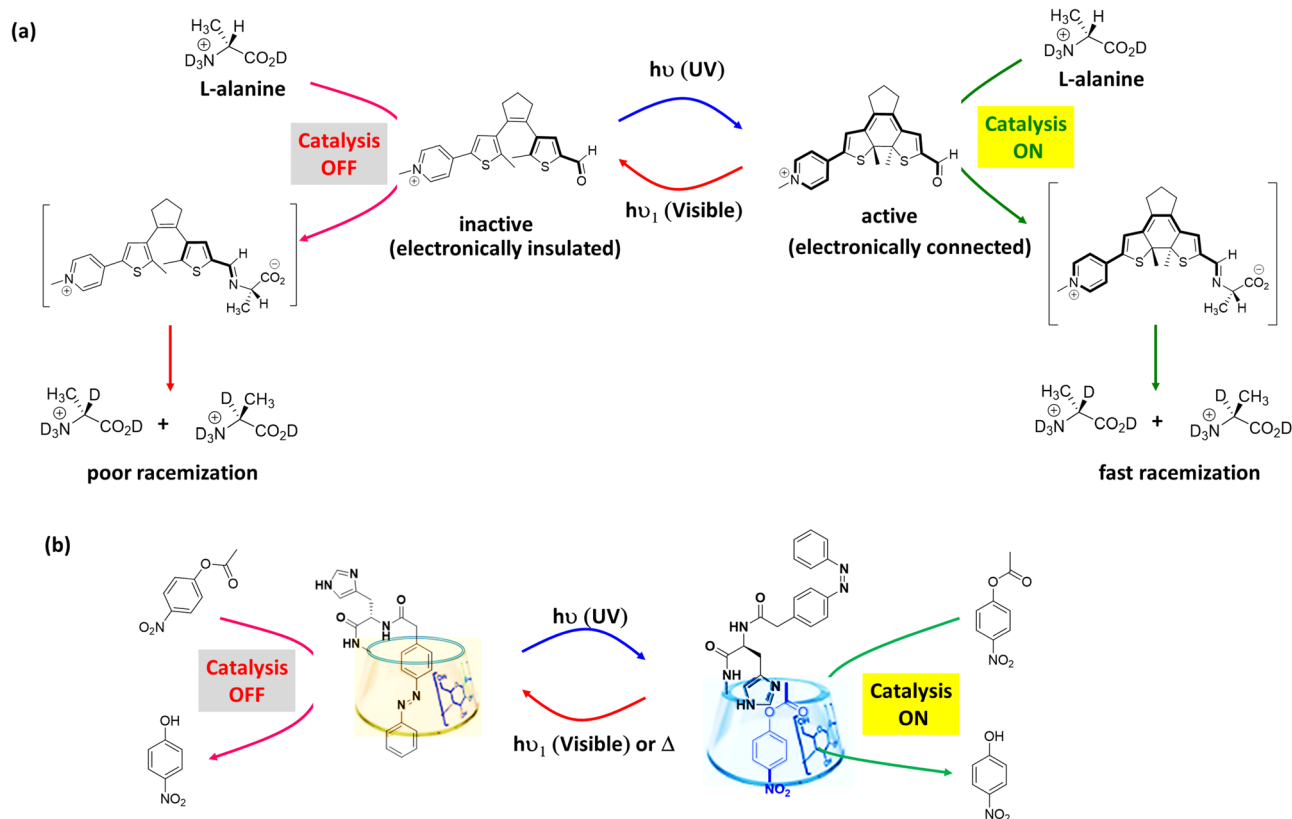


Fig. 5 Light-switchable catalytic systems. **a** Photoresponsive PLP mimic—Light-induced isomerization of dithienylethene structure between its “inactive” ring-opened and “active” ring-closed indicating whether the pyridinium and aldehyde are insulated or connected to each other for providing aldimine from reaction of aldehyde derivative and L-alanine. **b** β -cyclodextrin-based catalyst system—*trans*-azobenzene makes inclusion complex with the cavity of β -CD, resulting unavailability of catalytic site for the hydrolysis reaction. Light irradiation results *cis*-azobenzene that excluded from the cavity of β -CD allowing ester molecules to access the catalytic site in the cavity, which resulted faster hydrolysis. Adopted with permission from ref. ¹¹⁵, copyright 2001 WILEY-VCH Verlag GmbH, Weinheim, Fed. Rep. of Germany.

nature of the core and higher catalytic activity, which is presumably due to increase in substrate uptake and the greater mobility of the substrates within the core. In contrast, for CSC nanogel, the substrates were blocked to access the core presumably due to different-type of collapse for less-cross-linked PNIPAm shell. However, both systems, irrespective of the yields, showed high enantioselectivity for aldol product formation.

Exploiting thermoresponsive behavior of PNIPAm-based materials, metal NPs were entrapped into the polymeric network for the catalysis of various reactions in water^{85–89}. In these systems, metal NPs were stabilized by micelle forming amphiphilic block copolymers, and have been employed for a range of catalytic reactions such as hydrogenations, oxidations, reductions, and coupling reactions^{90–92}. An interpolymer interaction between the components at lower temperature and disruption of the interpolymer interaction at higher temperature result in this temperature-responsive dynamic nanoreactor system^{93–95}. However, colloidal nature of the catalytic sites and the challenges associated with the reversibility of catalyst activity and recycling limit, the use of these type of nanoreactors require further development⁹⁶.

Pickering emulsion (PE)-based catalytic system was reported by Dong et al.⁹⁷, which exhibited catalysis of dechlorination reaction as a function of temperature. In this example, PNIPAM was linked with UiO-66 (a nano-sized metal-organic frameworks (MOFs), where UiO-66 is an archetypal MOFs⁹⁸) emulsifier, where Pd nanoparticles (Pd-NPs) were incorporated to create a multicomponent composite emulsifier (Fig. 4a). The system was stabilized with toluene-in-water PE and supported biphasic

dechlorination reaction of chlorobenzenes (Table 1, Entry 27). Ammonium formate was used as the reducing agent. At 25 °C (below the LCST of polymer which is 32 °C), hydrophilic PNIPAM brushes stabilized the emulsions, and promoted interfacial catalytic activity of Pd-NPs for dechlorination of chlorobenzene derivatives. In comparison, at an elevated temperature (45 °C, above the LCST of polymer), PE system was demulsified as the PNIPAM brushes become hydrophobic and began to compact on the surface of the MOFs. It resulted organic and aqueous phase separation, which allowed product isolation from organic phase. Reducing temperature back to 25 °C leads to migration of MOFs to aqueous phase, which could be reused after re-homogenization. Thus, PE-based catalytic system could be switched between ‘on’ and ‘off’ just by varying temperature.

Besides polymer substances, supramolecular hydrogels can act as heterogeneous catalytic system, where reversible covalent self-assembly could be utilized for the development of catalyst systems that can be filtered out after completion of the reaction^{99–103}. These systems are interesting due to having large active surface, tunable catalytic activity, and well-ordered arrangement of catalytic groups, which can result enhanced efficiency. However, in most examples, the aldol reaction between pNB and cyclohexanone has been chosen as benchmark reaction¹⁰⁴. Metal nanoparticles can be embedded into supramolecular hydrogel structure and catalytic activity can be switched employing temperature stimulus. In an example, Léger et al.¹⁰⁵ developed cyclodextrin-based thermoresponsive hydrogel incorporating catalytically active ruthenium nanoparticles (Ru-NPs) for hydrogenation reactions (Fig. 4b). In this example, Ru-NPs were

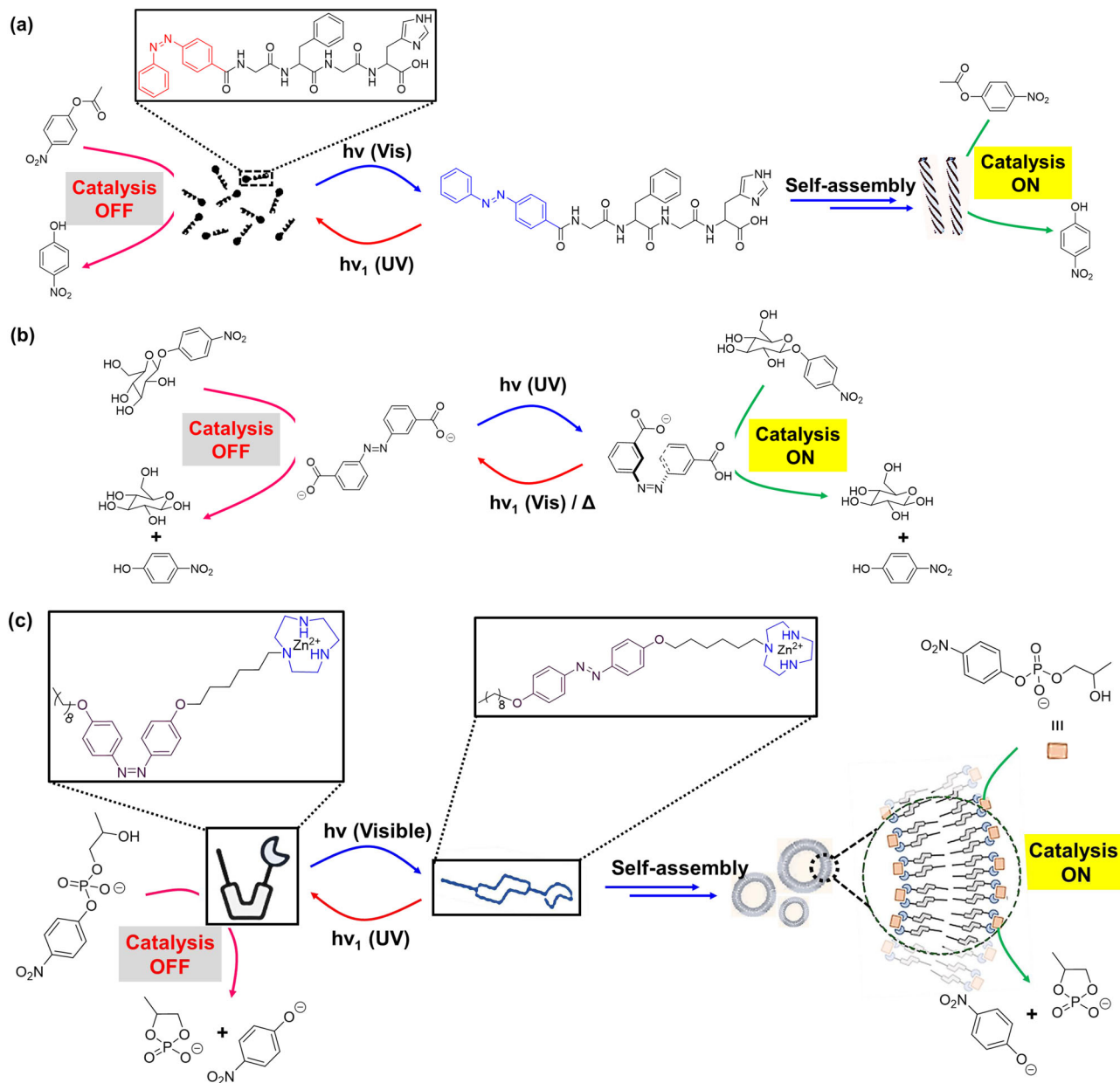


Fig. 6 Light-switchable catalytic systems based on cooperativity effect. **a** Peptide-based artificial hydrolase—azobenzene-functionalized peptide molecules can self-assemble into nanofibers, where basicity of imidazole is enhanced for hydrolase-like catalytic activity on pNPA. The activity can be switched ‘off’ under UV light irradiation via *trans* → *cis* photo-isomerization of the azobenzene group, leading to the disassembly of nanofibers. Adopted with permission from ref. ¹¹⁷, copyright 2018 Royal Society of Chemistry. **b** Photoswitchable glycosidase mimic – deprotonation of the carboxylic acid groups from *cis*-isomer of azobenzene-functionalized dicarboxylic acid occurs in a stepwise fashion, whereas deprotonation for *trans*-isomer occurs simultaneously. The monoanionic form of the *cis*-isomer can act as a glycosidase mimic that proceeds through a general acid-base catalytic mechanism for the hydrolysis of 4-nitrophenyl-β-D-glucopyranoside. Catalysis via the cooperative mechanism is absent for *trans*-isomer. **c** Photoswitchable self-assembled catalytic system—the catalysis can be switched between the ‘on’ and ‘off’ states by light irradiation. The *trans*-isomer of an amphiphile self-assembles into vesicular structures, which show cooperative catalysis for transphosphorylation reaction (Inset: *cis*- and *trans*-isomer of the amphiphile). UV light irradiation provides the *cis*-isomer, resulting disassembly and switching ‘off’ the catalysis. Adopted with permission from ref. ¹²³, copyright 2019 Wiley-VCH Verlag GmbH & Co. KGaA, Weinheim.

embedded into a supramolecular hydrogel matrix consisting N-alkylpyridinium amphiphile and α-cyclodextrin (α-CD). In water, the amphiphile and α-CD self-assembled to [3]pseudorotaxane, where the amphiphilic character of pyridinium-derivative was masked via alkyl chain inclusion into the cavities of α-CD, resulting in the formation of a hydrogel. At high temperature, the association constant between α-CD and the amphiphile become sufficiently low, resulting free pyridinium-

derivative and α-CD. Therefore, as a supramolecular carrier, α-CD influenced the mass transfer between NPs-containing aqueous phase and substrate-containing organic phase. Above the sol–gel transition temperature (39 °C), the system transformed to sol phase, where the catalytic hydrogenation of terminal alkenes took place (Table 1, Entry 28). The Ru-NPs, stabilized in the hydrogel network, demonstrated a pronounced catalytic activity at 50 °C. In contrast, after cooling the temperature to ambient

condition, the system spontaneously returned to the gel state, and showed no catalytic activity. However, the hydrogenated products and catalyst could be easily separated at lower temperature. It is worth noting that the dispersion of Ru-NPs in the hydrogel network remained intact for reuse.

Reversible nature of supramolecular gels by changing the temperature can allow a reversible sol–gel transition and thereby the modulation in catalysis. This type of tunable catalyst may find interesting applications, especially if different stimuli such as light, sound, magnetic field can be used to regulate hydrogel formation and subsequent catalysis.

Light-induced switchable catalytic systems

Light stimulus is advantageous over other stimuli due to its noninvasive nature, easy modulation via monitoring the source, and its precise physicochemical control over reaction¹⁰⁶. Photoresponsive processes found in nature illustrate the use of light irradiation for initiating and regulating complex molecular and biochemical processes. Different approaches can be employed in artificial photoresponsive systems^{107–109}, including photocatalysis, photoswitchable catalysis. In photocatalysis, upon light irradiation, an inactive precatalyst provides the catalytically active photoexcited state that reacts with a substrate, whereas a catalytically active species undergoes a reversible photochemical transformation in photoswitchable catalysis resulting the change in its intrinsic catalytic properties¹¹⁰. Photoswitchable catalysis offers distinct advantages over photocatalysis as the former provides an extra handle for controlling the catalyst activity. These photoswitchable catalytic systems are generally obtained via incorporating photoactive units in the molecular architecture. Electronic effect, steric effect, cooperative effect are the principal type of effects utilized to achieve control over these systems. In the following, we describe light-triggered switchable catalyst systems for organic transformations in aqueous environments.

Drawing inspiration from light-controlled biochemical process, controlling the catalytic activity via electronic modulation can be achieved. For example, pyridoxal-5-phosphate (PLP), which is biologically active form of vitamin B6, is a versatile enzyme cofactor used by nature for several biosynthetic procedure¹¹¹. The action of PLP depends on the electronic connection between aldehyde group and pyridinium group. The pyridinium group in the aldimine (formed by the condensation of an amino acid and PLP) enhances the acidity of the α -hydrogen by stabilizing the conjugate base through contributions from the quinonoid structure. A photoresponsive mimic of PLP was demonstrated by Wilson et al.¹¹², where diarylethene photoswitch was replaced in the PLP core ring. In the ring-opened isomer, the pyridinium and aldehyde functional groups were electronically insulated, which precluded catalytic activity (Fig. 5a). On the other hand, irradiation of UV light ($\lambda = 365$ nm) provided fully conjugated ring-closed form, where aldehyde and pyridinium groups are electronically connected. Therefore, the ring-closed form provides the stabilized quinonoid structure upon condensation with L-alanine (an amino acid), and deprotonation of the aldimine α -hydrogen. Thus, treatment of L-alanine with ring-opened isomer resulted in poor racemization reaction (3% yield), whereas an increase in the rate of racemization was observed upon UV irradiation to ring-closed form (Table 1, Entry 29). The ability of light-responsive PLP mimic, as a controllable catalyst, was demonstrated employing hydrogen–deuterium exchange experiments in a mixture of D_2O and CD_3CO_2D . Furthermore, reversible switching the catalytic activity between its opened-form (catalysis ‘off’) and its closed-form (catalysis ‘on’) was demonstrated through alternate exposure to UV ($\lambda = 365$ nm) and visible light ($\lambda > 490$ nm).

The *trans* \rightarrow *cis* isomerization of an azobenzene or stilbene moiety can be used for catalytic purpose in aqueous media enabling steric modulation via large geometrical change due to the isomerization process. In these systems, the active site of the catalyst would be inaccessible to the reactants by a group such as host–guest binding, bulky functional group to shield the catalytic sites. Light-induced isomerization would result the geometrical change and unblocking of catalytic site to the reactants. In an early example, Ueno et al.¹¹³ exploited host–guest interactions to modulate the catalytic activity, where β -cyclodextrin (β -CD) acts as host and 4-carboxyazobenzene acts as guest. The azobenzene derivative changes the rate of the hydrolysis of pNPA in tris buffer medium (pH 8.7) (Table 1, Entry 3). Complexation between *trans*-azobenzene moiety and β -CD effectively block one end of β -CD, resulting inaccessible β -CD for the ester substrate, and thereby inhibition of hydrolysis (rate constant, $K = 1.17 \times 10^{-4} S^{-1}$ for uncatalyzed reaction). However, upon irradiation of UV light ($\lambda = 365$ nm), *trans* \rightarrow *cis* isomerization led to exclusion of *cis*-azobenzene moiety from β -CD, which resulted inclusion of pNPA in the cavity of β -CD. This facilitates attack of one of the peripheral hydroxyl groups of β -CD on the ester moiety. Therefore, enhancement in the rate of hydrolysis (rate constant, $K = 1.56 \times 10^{-4} S^{-1}$ for catalyzed reaction) was observed. Moreover, *cis*-azobenzene moiety can isomerize back to *trans*-azobenzene moiety utilizing thermal energy or irradiation of visible light, resulting the inhibition in ester hydrolysis rate. Likewise, photoswitchable catalysts were developed based on covalently attached azobenzene moieties to the lower rim of β -CD¹¹⁴. Photocontrolled imidazole catalyzed hydrolysis of esters in phosphate buffer (pH 7.2) was reported by Lee et al.¹¹⁵ employing a functionalized β -CD with an azobenzene unit and a histidine residue (Table 1, Entry 4). In this example, an imidazole group was attached to an azobenzene-based pendant and the catalytic site is unavailable for the ester molecules as *trans*-azobenzene effectively makes inclusion complex with host cavity of β -CD (Fig. 5b). Conversely, light irradiation results *cis*-azobenzene, which could not be included in the cavity of β -CD and hence the binding site is available for the insertion of both the ester molecule and imidazole moiety, resulted faster hydrolysis of various ester molecules, namely pNPA (kinetic efficiency = $0.27 s^{-1} M^{-1}$), Boc-L-alanine-*p*-nitrophenyl ester (kinetic efficiency = $1.0 s^{-1} M^{-1}$) and Boc-D-alanine-*p*-nitrophenyl ester (kinetic efficiency = $0.96 s^{-1} M^{-1}$). Furthermore, the azobenzene moieties were functionalized to gold nanoparticles (Au-NPs) that bind Zn^{+2} coordinated β -CD dimer as a heterogeneous photoswitchable system to modulate ester hydrolyses¹¹⁶. Upon complexation, the NPs aggregated and showed poor catalytic activity (rate constant, $k = 54.1 \times 10^{-8} M \text{ min}^{-1}$ for *trans*-isomer). UV light irradiation led to *trans* \rightarrow *cis* isomerization, resulting exclusion of *cis*-azobenzene moiety from β -CD. NPs deaggregation and enhancement in ester hydrolysis rate were observed (rate constant, $k = 132 \times 10^{-8} M \text{ min}^{-1}$ for *cis*-isomer). These, light-induced switching of catalytic activity is an excellent example with respect to artificial molecular switching systems in aqueous medium.

Regulation of enzyme-like catalytic activity could be achieved in artificial systems by introducing flexible domains in photoswitchable systems for enabling preorganization and induced fit. In an example, Zhao et al.¹¹⁷ reported an artificial photoswitchable hydrolase activity by incorporating an azobenzene group to peptide sequence Gly-Phe-Gly-His (GFGH) (Fig. 6a). The peptide can self-assembled into nanofibers, by which basicity of the imidazole functional group of histidine was enhanced based on the cooperative effects. The hydrophobic microenvironment in the supramolecular assemblies was suitable for the hydrolase-like catalytic activity on pNPA in PBS buffer (pH 7.4) (kinetic efficiency = $13.95 \times 10^{-3} \text{ min}^{-1} \text{ mM}^{-1}$ for *trans*-isomer) (Table 1,

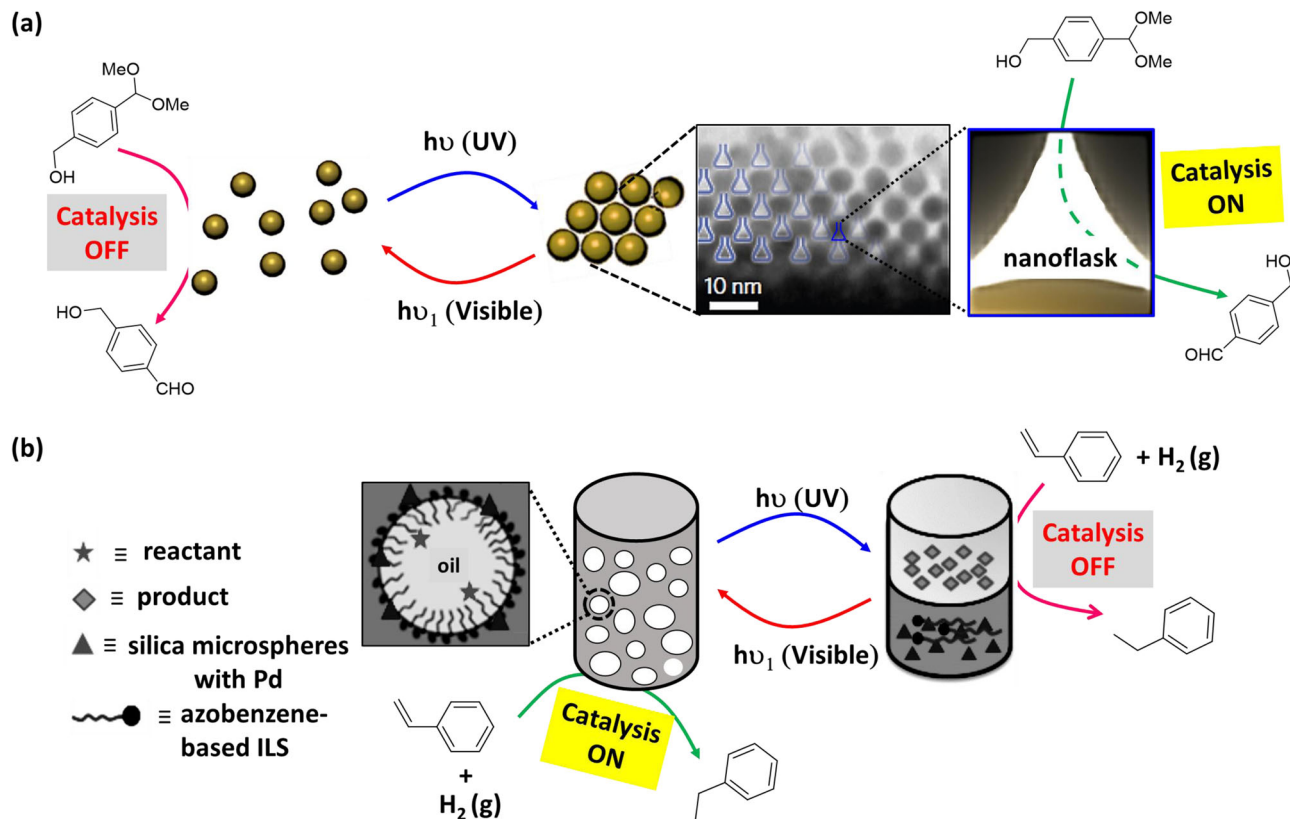


Fig. 7 Light-switchable nanoparticle-based catalytic systems. **a** Light-triggered dynamic formation of 'nanoflasks' based on azobenzene-functionalized Au-NPs—upon UV irradiation, *cis*-isomer aggregated to provide the nanoflask, which provide suitable atmosphere for acetal hydrolysis. Visible-light-triggered *trans*-isomer disintegrated the nanoflask and consequently switching 'off' the catalysis. Adopted with permission from ref. ¹²⁷, copyright 2015, Nature Publishing Group. **b** Light-switchable PE-based system—*trans*-azobenzene-based catalytic system efficiently catalyzes hydrogenation reaction at ambient condition. UV irradiation results phase separation and switching 'off' the catalysis, whereas visible light irradiation and homogenization results emulsification for catalytic reaction. Adopted with permission from ref. ¹²⁸, copyright 2020 Wiley-VCH GmbH.

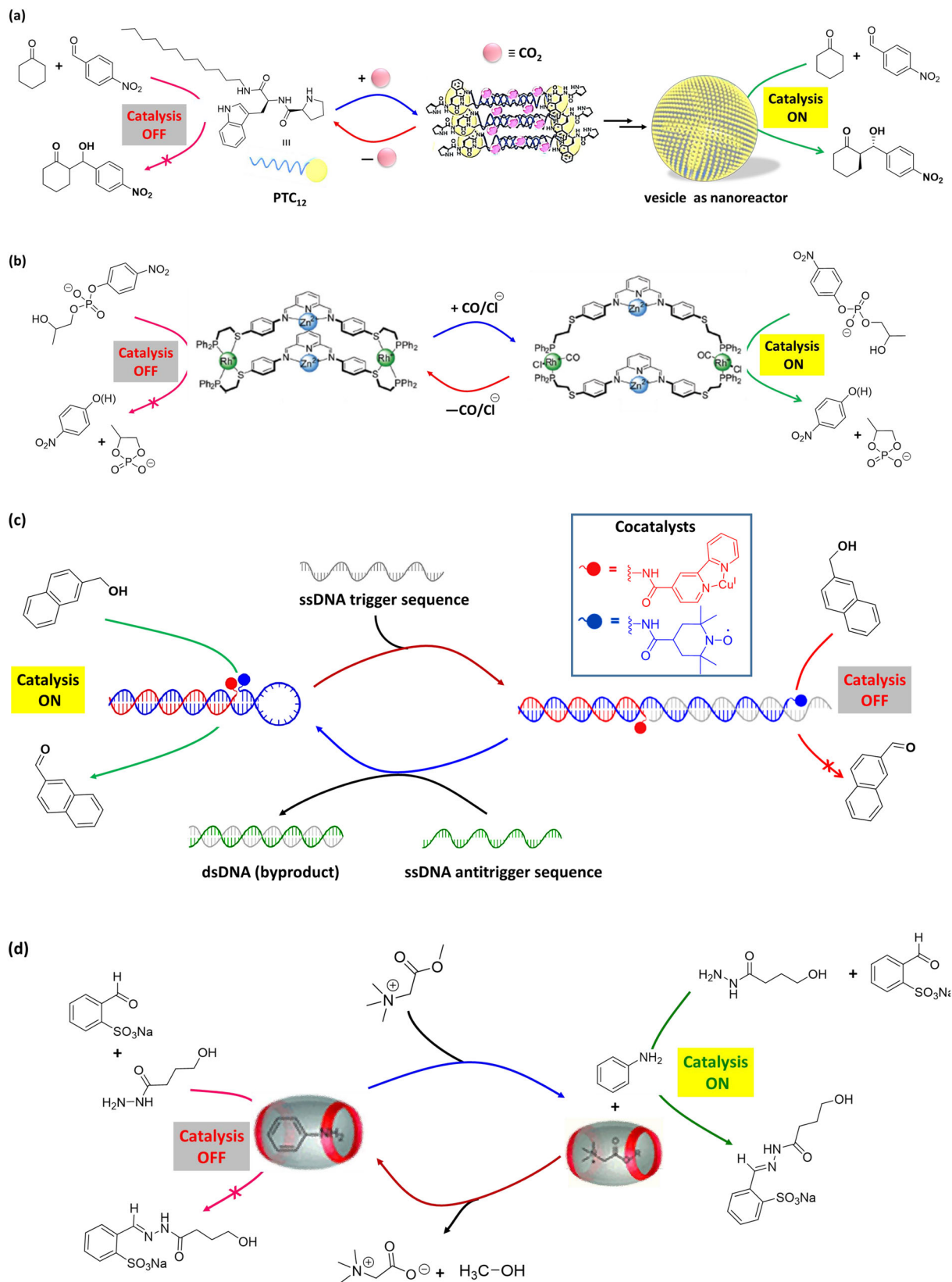
Entry 5). Upon UV irradiation, the azobenzene moiety isomerizes to *trans* → *cis* conformation, resulting break down of β -sheet nanofibers to random coils and consequent reduction in catalytic efficiency (kinetic efficiency = $11.08 \times 10^{-3} \text{ min}^{-1} \text{ mM}^{-1}$ for *cis*-isomer). This way, the activity of the hydrolase mimic can be switched reversibly employing UV and visible light. However, repeated cycles of activation and deactivation via light irradiation appeared to disturb the supramolecular architecture, and reduction in catalytic ability.

Due to light-induced isomerization process, a change in the distance or orientation of catalytic sites of switchable catalyst can modulate the rate of chemical process¹¹⁸. Artificial photoresponsive glycosidase mimic was reported by Samanta et al.¹¹⁹ employing a photoresponsive bifunctional organocatalyst based on the cooperative effects of azobenzene-functionalized biscalboxylic acid (Fig. 6b). Glycosidase enzyme is responsible for hydrolysis of glycosidic bond between two glucose residues of biopolymers¹²⁰. One of the carboxyl groups of glycosidases functions as general acid catalyst, whereas other carboxylic group acts as a nucleophile, forming a covalent glycosyl-enzyme intermediate. In the glycosidase mimic, the carboxylic acid groups of *trans*-azobenzene isomer ionize at roughly same pH, whereas deprotonation of *cis*-azobenzene isomer, which is obtained via 366 nm light irradiation, occurs in a stepwise fashion and it exists as the monoanionic species between pH 4.7 and 6.5. An increase in the reaction rate of six order was observed with respect to background reaction at pH 5.8 for the hydrolysis of 4-nitrophenyl- β -D-glycopyranoside (kinetic efficiency = $9.2 \times 10^2 \text{ mM}^{-1} \text{ min}^{-1}$) (Table 1, Entry 30), which is similar in terms of functionality as the active form of a

glycosidase. Moreover, the catalytic activity could be switched 'on/off' via altering exposure to UV/visible light.

The carbonic anhydrase (CA) enzymes catalyze the reversible hydration or dehydration of $\text{CO}_2/\text{HCO}_3^-$. It consists a distorted tetrahedral Zn(II) complex coordinated to imidazole nitrogen atoms of histidine residues and a water molecule¹²¹. Photoresponsive CA enzyme mimic was reported by Saha et al.¹²² for pNPA hydrolysis, where the CA-activity can be turned 'on/off' reversibly by irradiation of light in PBS Buffer (pH = 7.6) (Table 1, Entry 7). This example employed a photoregulated CA mimic with Zn(II) complex of two imidazoles appended azobenzene system. The *cis*-azobenzene isomer formed a 1:1 complex with Zn(II) ions that showed efficiency as an active-site mimic of the CA enzyme (kinetic efficiency = $0.24 \text{ mM}^{-1} \text{ min}^{-1}$). In contrast, the *trans*-isomer provided a polymeric —(Zn(II)-*trans*-)— network, which showed poor efficiency towards hydrolysis reaction of pNPA.

Artificial catalysts have the potential for controlling catalysis within self-assembled structures via the combination of cooperativity and self-assembled structure formation. In an example, Ren et al.¹²³ reported self-assembly of azobenzene-based amphiphilic molecules for creating catalytic pockets utilizing intermolecular cooperative effect that can be switched between 'on/off' states via light irradiation. In this example, azobenzene-functionalized 1,4,7-triaza-cyclononane (TACN) derivative self-assembled into vesicular structures in a HEPES buffer solution (pH 7) (Fig. 6c). The molecular assembly can effectively catalyze the transphosphorylation reaction (rate = $\sim 0.5 \times 10^{-8} \text{ mol s}^{-1}$ for *trans*-isomer) of 2-hydroxypropyl-4-nitrophenylphosphate (HPNPP), which is a model substrate for RNA hydrolysis (Table 1, Entry 31).



UV light irradiation ($\lambda = 365$ nm) converts *trans* \rightarrow *cis*-isomer, resulting disassembled states and poor catalytic activity (rate = $\sim 0.17 \times 10^{-8}$ mol s $^{-1}$ for *cis*-isomer). Moreover, conversion of *cis* \rightarrow *trans*-isomer and thereby the assembled state could be obtained via light irradiation from a white LED lamp. Thus, light

irradiation within the amphiphilic molecule can allow switching between assembled and disassembled states, thereby modulating the rate of chemical transformations. Likewise, the polarity change in 4-(phenylazo)-benzoate derivative due to light irradiated *trans* \leftrightarrow *cis* isomerization was utilized by Neri et al.¹²⁴ for

Fig. 8 Small molecule-responsive switchable catalytic systems. **a** CO₂-responsive switchable system—amphiphilic molecule, PTC₁₂ is insoluble in water and catalytic aldol reaction is switched 'off'. In presence of CO₂, PTC₁₂ self-assembles to vesicle nanoreactor, where catalysis is turned 'on' for efficient aldol reaction. Adopted with permission from the ref. ¹³⁴, copyright 2013 WILEY-VCH Verlag GmbH & Co. KGaA, Weinheim. **b** Small molecule/ion-induced supramolecular allosteric catalyst—use of small molecule regulators (CO and Cl⁻) change the size of the macrocycle, the accessibility to the active binuclear Zn site, and thereby the catalysis of HPNP hydrolysis reaction. Adopted with permission from the ref. ¹⁴⁰, copyright 2007, American Chemical Society. **c** DNA duplex-scaffold functionalized with Cu-bpy and TEMPO for switchable catalysis—the distance between the two cocatalysts in DNA architecture can be altered upon introduction of ssDNA strand (Inset: structures of Cu(I)-bpy and TEMPO cocatalysts). Presence of an ssDNA trigger sequence, the structure holds the cocatalysts apart and turning 'off' the catalysis. The original catalyst conformation is restored upon addition of an ssDNA antitrigger strand that catalyze the oxidation of 2-naphthalenemethanol in borate buffer (pH 9.5) environment. Adopted with permission from ref. ¹⁴³, copyright 2021, American Chemical Society. **d** Chemical fuel-induced transient availability of catalyst for a chemical reaction—glycine betaine methyl ester competes for CB[7] binding with aniline, and their hydrolysis controls the release of aniline from CB[7] for hydrazone formation reaction. Glycine betaine methyl ester binds with CB[7], allowing the release of aniline and turning 'on' the catalysis. Rebinding of aniline in the cavity of CB[7] due to decay of ester molecules switch 'off' the catalysis. Adopted with permission from ref. ¹⁶⁵, copyright 2022 American Chemical Society.

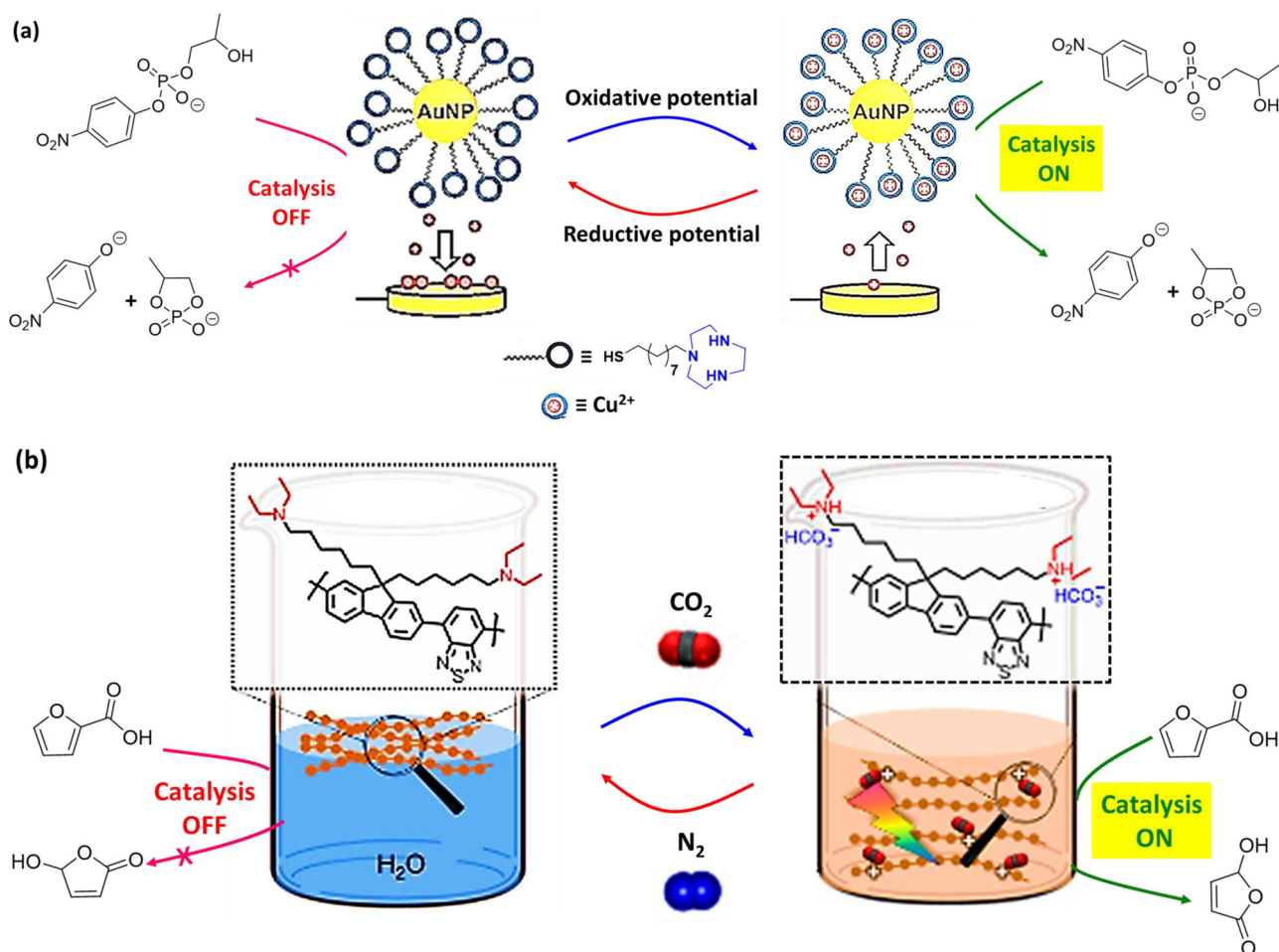


Fig. 9 Other stimuli-switchable catalytic systems. **a** Electrochemical-induced switchable catalyst stem—activation and deactivation of Au-NP-based supramolecular nanocatalyst via electrochemical stimulus for the hydrolysis of HPNPP. Adopted with permission from the ref. ¹⁷⁰, copyright 2016 WILEY-VCH Verlag GmbH & Co. KGaA, Weinheim. **b** Polymer photocatalyst via switchable hydrophilicity by CO₂/N₂ swing—in presence of CO₂, photocatalyst generates a hydrophilic structure that enables the catalyst to support photo-oxidation of 2-furoic acid in water. On purging in N₂ into the system, CO₂ is released from the system and the photocatalysts clusters back to its original hydrophobic nature, terminating the catalytic activity and the reaction (inset: the structure of photocatalyst in absence/presence of CO₂). Adopted with permission from ref. ¹⁷³, copyright 2018 Wiley-VCH Verlag GmbH & Co. KGaA, Weinheim.

controlling the binding affinity to Au-NPs and thereby their catalytic activity. In this example, the Au-NPs were functionalized with a monolayer of alkyl thiol terminated with aTACN—Zn²⁺ headgroup, which can catalyze the transphosphorylation of HPNPP in aqueous buffer (pH 7.0) (Table 1, Entry 32). Light-sensitive 4-(phenylazo)-benzoate was used as a cofactor to regulate the catalytic activity of the nanosystem. The catalytic activity was downregulated with the *trans*-azobenzene derivative which was

attributed to its higher binding affinity to the catalyst. In contrast, the *cis*-azobenzene derivative disfavored its hydrophobic binding with the apolar part of the Au-NP-attached monolayer due to the increased polarity, and increased the reaction rate up to 1.5-fold. Although several operational limitations of this system were reported, but reversible formation of cooperative catalysts within a dynamic self-assembled system is a promising new tool for the design of complex artificial systems in aqueous environment.

Self-aggregation of NPs could provide suitable hydrophobic inert environment amidst surrounding aqueous medium^{125,126}. In a seminal work, Zhao et al.¹²⁷ described novel class of synthetic confined environments, whose formation and disassembly are governed by light irradiation. In this example, azobenzene-functionalized Au-NPs were used for reversibly creating and destroying confined environments ('nanoflasks'), where trapped molecules can undergo chemical reactions with increased rates (Fig. 7a). Upon UV light irradiation, *trans* → *cis* isomerization of azobenzene moiety paves the pathway for aggregation of the NPs and formation of nanoflasks where reaction rate increases. Afterwards, exposure of visible light results *cis* → *trans* isomerization and subsequent disintegration of the 'nanoflasks' assuring product recovery at the desired yield. Acid-catalyzed hydrolysis of acetal to aldehyde in water-saturated toluene in presence of functionalized Au-NPs was investigated (Table 1, Entry 35). The reaction was observed to have proceeded at much higher rates as compared to that in absence of the aggregates or UV irradiation.

Azobenzene photoswitches were employed in regulating the stabilization of Pickering emulsions (PEs) and catalysis in such systems. In an example, Li et al.¹²⁸ reported light-induced emulsification and demulsification of ionic liquid surfactants for catalytic hydrogenation of styrene (Fig. 7b). The PE was stabilized by silica microspheres functionalized with surface-loaded Pd and water-soluble azobenzene-based ionic liquid surfactant (ILS). Catalytic system Pd/SiO₂/ILS was found to actively participate in catalytic hydrogenation of styrene with excellent conversion at ambient condition (Table 1, Entry 21). Upon UV light irradiation, *trans* → *cis* isomerization of azobenzene moiety resulted increase in hydrophilicity of ILS and decrease of surface activity, consequently destabilization of emulsion. A complete phase separation of aqueous phase and organic phase provided poor rate of catalytic reaction, but ease of product separation. Moreover, irradiation of visible light to the system, followed by homogenization, reformed the stable PE for reuse. Thus, PE can be used as a microreactor, which allowed controlled catalytic reaction, product separation, and catalyst recycling just via alternate exposure to UV and visible-light irradiation.

Light-induced reversible change in wettability of TiO₂ surfaces has been utilized in photoswitchable heterogeneous catalysis. In presence of UV light, water molecule (present in moisture) can coordinate with the titanium atom of a TiO₂ surface, which resulted increase in number of -OH groups, and the hydrogen bonding ability of the surface¹²⁹. Thus, the number of -OH groups of a surface could be modulated via UV light irradiation and keeping in the dark. Various hydrogen bond catalyzed organic reactions were observed on these surfaces, including epoxide ring-openings (33–38% yield under UV irradiation, whereas 0–9% yield in dark), cycloadditions (54–76% yield under UV irradiation, whereas 30–34% yield in dark), and C–C forming reactions (64% yield under UV irradiation, whereas 18% yield in dark). The reversible wettability was also employed for switching the rate of aldol reaction between benzaldehyde and acetophenone. Thus, a broad range of C–C bond-forming chemical reactions could be modulated by using heterogeneous catalysts, such as TiO₂ via light irradiation.

Small molecule-induced switchable catalytic systems

Self-assembly of amphiphilic molecules in water can provide nano- or microstructures such as micelles, vesicles, and emulsions, which can be used as nanoreactors by offering suitable reaction space from the environment^{130–133}. However, controlling and regulating these nanoreactors dynamically and reversibly employing small molecules is a great challenge.

Compressed CO₂ can trigger the formation of nanoreactors such as nanoemulsion. Reversibility between micelle-to-vesicle transitions can be controlled by regulating the pressure of CO₂ and eventually the activity and selectivity of a catalyst. Qin et al.¹³⁴ employed a proline-based amphiphilic molecule (PTC₁₂, Fig. 8a) having a long alkyl chain at the C-terminus to form vesicle under compressed CO₂. The peptide-based amphiphilic PTC₁₂ was insoluble in water. However, upon introduction of compressed CO₂, PTC₁₂ formed bicarbonate salt that increases the hydrophilicity of PTC₁₂ and consequently facilitates the formation of vesicular assembly in water. The hydrogen bonds between amide functionality among head groups reduced the surface area per surfactant headgroup, resulting the formation of vesicles. Besides, compressed CO₂ regulated the size of the vesicles via inserting CO₂ into the hydrophobic area of the packed amphiphiles. The vesicle structures can catalyze a direct aldol reaction with high selectivity (99% yield, 93% ee) (Table 1, Entry 14). Moreover, the nanostructures were regulated by the presence of CO₂, providing a dynamic regulation of the system where the catalyst activity and selectivity can be controlled. The amphiphilic proline derivative could be reused to form the vesicles for catalyzing the reaction. Such process could be done several times just via alternate exposure of CO₂ to the system or by removing CO₂ from the system. This is an interesting example that bridge the gap between random and unstable catalytic emulsion systems and the ordered and stable catalytic hydrogels via employing small molecule such as CO₂.

Nature has evolved suitable pathways for controlling the hydrolysis of phosphate diesters in important biomolecules such as DNA and RNA. Many of the enzymes, such as P1 nuclease, DNA polymerase I, phospholipase C, and alkaline phosphatase, depend on the synergistic action of two metal centers (typically Zn²⁺) for promoting the hydrolytic cleavage of the phosphate diester bonds^{135,136}. In artificial systems, allosteric control over switchable catalysis has emerged in recent years via the use of (nano)mechanical reorganizations^{137–139}. In an example, Yoon et al.¹⁴⁰ described a switchable catalytic system having Zn(II)-pyridine-bisimine catalytic motifs. The system can undergo reversible switching triggered by the addition or removal of chloride ion (Cl⁻) and carbon monoxide (CO) in a pseudo-aqueous solution (Table 1, Entry 33). The hydrolysis of HPNP (Fig. 8b) could be turned 'on/off' in the networked system employing a metalation/demetalation protocol, where weak-link approach (WLA)¹⁴¹ is exploited. No conversion was observed in the closed state of the catalyst (catalysis 'off'), while the open state led to full conversion (catalysis 'on'). The absence of activity in the 'off' state was ascribed to the short distance between Zn atoms that inhibited the bimetallic intramolecular reaction. On the other hand, the presence of monodentate ligands (CO or Cl⁻) at rhodium (Rh) centers allowed a switch to a flexible semi-open form as 'on' state from a rigid-closed form as 'off' state. The semi-open structure can be switched back to the rigid-closed form just by removal of these monodentate ligands.

Artificial synergistic catalysis, combining two cocatalysts in close proximity, work in concert for carrying out a reaction, which could not be possible employing either cocatalyst alone¹⁴². Recently, Pimentel et al.¹⁴³ demonstrated DNA-based scaffold for switchable synergistic catalysis through tuning the geometric relationship between the cocatalysts (Cu and 2,2,6,6-tetramethylpiperidine-1-oxyl [TEMPO]) for oxidation of naphthalenemethanol in aqueous borate buffer (pH 9.5) medium (1/1 borate buffer/acetonitrile) (Table 1, Entry 36). In this example, DNA-cocatalyst conjugates were prepared via bioconjugation of two cocatalysts (Cu and TEMPO) to the end of a DNA helix (Fig. 8c). DNA duplex was obtained via self-assembly of DNA-cocatalyst conjugates that shows

much better catalytic activity compared to unscaffolded cocatalysts (without DNA duplex). This is due to the precise placement of the cocatalysts in the DNA duplex. Moreover, the DNA backbone allowed the switching of catalytic activity exploiting a strand-displacement approach. A dynamic DNA structure was created just by incorporating a hairpin motif into the sequence of one of the cocatalyst conjugates. In presence of a trigger sequence, complementary to the hairpin motif, the structure opens up, where distance between the cocatalysts is increased. As a result, synergistic catalysis is turned 'off'. When a corresponding antitrigger sequence is added, the original catalyst conformation can be restored via formation of dsDNA as by product, and catalytic activity could be restored. The DNA-scaffolded cocatalysts exhibited activity in the oxidation of 6-methoxy-2-naphthalenemethanol (a fluorogenic probe). Thus, synergistic catalytic activity can be controlled through conformational switching of DNA triggered by chemical stimuli. Regulation of enzyme activity in response to environmental conditions is critical to many metabolic functions. Mimicking enzyme regulatory of nature, scientists are creating artificial nanoreactors for potential applications ranging from diagnostics to the production of artificial (smart) materials^{144–146}. On this regard, chemistries involving protein–DNA conjugation provide the precession in positing proteins and other biomolecules on DNA scaffolds to modulate intermolecular interactions and the local environment^{147–149}.

In nature, living systems have complex dissipative cellular networks, where advanced functions such as adaptability, responsiveness are feasible through energy consumption. Likewise, artificial dissipative chemical systems, which is out-of-equilibrium assemblies require inputs of energy in the form of chemical fuels^{150–154} or light^{155,156} to stay in a functional state. Out-of-equilibrium state of a synthetic molecular machine can be used to control catalysis¹⁵⁷. In an interesting work, Maiti et al.¹⁵⁸ demonstrated transient availability of vesicular nanoreactor for enhancing the rate of a nucleophilic aromatic substitution reaction. Assembly of the vesicle nanoreactor was driven by the electrostatic complexation of anionic adenosine triphosphate (ATP) to a cationic surfactant, whereas potato pyruvate kinase enzyme hydrolyses ATP to adenosine monophosphate (AMP) leading to breakdown of the formed vesicles. The transient presence of the vesicles was used as nanoreactor to accelerate the reaction rate between 4-chloro-7-nitrobenzofurazan and 1-octanethiol in HEPES buffer (pH 7) as it provides suitable reaction environment, however, there is no catalyst is involved. In contrast, there is no effect on the reaction in presence of only the cationic surfactant or just ATP. This system could in principle be applied for many chemical reactions, because the only requirement is the hydrophobicity of the reactants¹⁵⁹. Small biomolecule, such as ATP-induced temporal control over chemical reactivity in artificial synthetic system provided the dissipative catalyst systems as the basis for many events in biology^{157,160–163}. In another example, Biagini et al.¹⁶⁴ reported a molecular machine where rotaxane can be transiently changed from a catalytically inactive form into an active state by $\text{CCl}_3\text{CO}_2\text{H}$. Deprotonation by the rotaxane helped decarboxylation of the acid group, thereby bringing the system to its original state and stopping catalysis. However, the system works in organic solvent (CH_2Cl_2 or toluene). Recently, van der Helm et al.¹⁶⁵ reported cucurbit[7]uril (CB[7]) as a supramolecular host to encapsulate aniline (catalyst molecule) in an aqueous environment, which can be released via addition of hydrolytically unstable esters as chemical fuel (Fig. 8d). Addition of glycine betaine methyl ester, as chemical fuel, resulted favorable binding toward CB[7], leading to expulsion of aniline from the cavity of CB[7]. In phosphate buffer (pH 7.5), aniline catalyzed hydrazone formation reaction between 2-formylbenzenesulfonate and a hydrazide derivative to form

hydrazone product (Table 1, Entry 38). However, since the ester molecules are unstable under aqueous condition, they hydrolyze to corresponding acid and methanol, which are nonbonding to the cavity of CB[7]. As a result, aniline rebinds in the host cavity of CB[7], and switching 'off' the catalysis. Availability of aniline for catalyzing the reaction depends on the lifetime of ester molecule in aqueous environment. Thus, transient presence of a chemical fuel that can bind to a supramolecular host and expel a catalyst, can turn 'on' catalysis. An advantage of such catalytic system is that it could, in principle, be applied for many chemical reactions by altering the structure of catalyst and chemical fuel of different concentrations.

Electrochemical-switchable catalytic reactions

Application of electrochemical methods for synthesis of organic compounds in aqueous medium are very appealing from both an economic and an ecological point of view^{166,167}. Electrochemical-induced activation/deactivation of inorganic and organic hybrid nanomaterials is a promising strategy as enzyme mimic for chemical transformations of organic molecules¹⁶⁸. However, it is challenging to regulate these systems reversibly in aqueous environments. Au-NPs have been used for catalysis of transphosphorylation of HPNPP, which is a model compound used for mimicking RNA hydrolysis¹⁶⁹. Employing electrochemical input, della Sala et al.¹⁷⁰ reported reversible activation and deactivation of Au-NP-based supramolecular nanocatalyst in aqueous buffer (HEPES buffer, pH = 7.0). In this example, Au-NPs were covered with C_9 -thiols terminating with TACN head group and electrochemical controlled association/dissociation of metal ions have been used as a regulatory mechanism for catalysis (Fig. 9a). The electrochemical input in the form of oxidation potential generated Cu(II) coordinated Au-NP, which can switch on the transphosphorylation of HPNPP (Table 1, Entry 34). In contrast, application of reductive potential resulted $\text{Cu}^{2+} \rightarrow \text{Cu}^0$ conversion and redeposition onto the electrode surface. This provided copper-free Au-NP (inactive catalyst) to switch 'off' transphosphorylation of HPNPP. Likewise, electrochemistry can be used as effective and clean tool for the regulation of the catalytic activity of a supramolecular catalyst.

Other stimuli-induced switchable catalytic systems

Multi stimuli-switchable systems in aqueous environments provide smart tunability in catalytic activity for organic transformations. In this regard, conjugated polymers, metal-organic frameworks have been employed by attaching stimuli-responsive functional groups for photocatalytic reactions in aqueous media^{171,172}. In an example, Zhang et al.¹⁷³ employed conjugated poly(bisthiophene) (PBT) for photocatalytic oxidation of 2-furoic acid into 5-hydroxy-2(5H)-furanone in aqueous medium (Table 1, Entry 39). In this example, PBT was functionalized with diethylamine (DEA), which is hydrophobic in nature. On introducing CO_2 in the system, carbonic acid was generated and solubilized in aqueous medium, which can successfully perform visible-light-induced catalytic reactions (Fig. 9b). On purging the system with nitrogen, CO_2 desorbs from the system and turns the polymeric segment back to its hydrophobic nature that stops the reaction and can be utilized to separate the product. Therefore, product formation is only feasible in presence of light and CO_2 stimulus. The reversible switchability of polar nature for the polymeric segment in water was used for photocatalytic reduction of 4-nitrophenol to 4-aminophenol in presence of NaBH_4 (Table 1, Entry 19), and visible-light-induced coupling of caffeine and aryldiazonium tetrafluoroborate as radical-mediated arylation of heteroarene (Table 1, Entry 40).

Application of magnetic field for controlled organocatalysis in water is scarce. However, magnetic materials (nanoparticles) functionalized with organocatalysts have been employed for various organic transformations in aqueous environments due to their easy recovery and reuse^{174,175}. In such systems, the magnetic core provides a magnetic function and the functionalized shell participates in catalysis. An interesting example exploiting thermoresponsive behavior of PNIPAM was described by Wang et al.¹⁷⁶, where proline-based nano hybrid was prepared by grafting thermoresponsive PNIPAM fragment and magneto-sensitive vinyl modified Fe₃O₄@SiO₂. In this example, PNIPAM fragment remained in dissolved state below the LCST (38 °C) due to the hydrophilic nature of PNIPAM and therefore catalytically inactive. In contrast, the PNIPAM turned hydrophobic at a higher temperature, resulting the nano hybrid aggregation to ‘broom-type’ corona that provided the hydrophobic microenvironment for catalyzing the aldol reaction of cyclohexanone and pNB (94% yield, 95% ee) (Table 1, Entry 15). Thereafter, magnetic responsiveness allowed to recover the nano hybrid material from the reaction mixture by application of an external magnetic field. Likewise, magnetic- and CO₂-dual-responsive Pickering emulsion (PE)-based catalyst system was reported by Tang et al.¹⁷⁷ employing Fe₃O₄ and DEA, which provides a switchable catalytic platform for the benzyl alcohol oxidation. Catalytic system was prepared by introducing DEA for CO₂ responsiveness, Fe₃O₄ for magnetic responsiveness, and tetramethyl-4-piperidylmethacrylate (TMPM) as TEMPO precursor. As a biphasic reaction, the Anelli system (NaClO/NaBr/TEMPO)¹⁷⁸ was employed for benzyl alcohol oxidation in water-in-oil PE. This catalyst system provided full conversion for benzyl alcohol (Table 1, Entry 37) and excellent yields (>94%) for other aromatic alcohols (diphenylmethanol, 2-phenylethanol, 4-nitrobenzyl alcohol) and aliphatic alcohols (cyclohexanol, 1-nonanol, 1-hexanol). Thereafter, bubbling of CO₂ resulted protonation of the tertiary amino groups. As a consequence, demulsification happened due to formation of relatively hydrophilic tertiary amino groups, which desorbed from the interface and switching ‘off’ the catalysis. They can be quickly gathered under magnetic field, followed by purging of N₂ results deprotonation of the tertiary amine group and formation of PE for reuse. Likewise, use of an external magnetic field provides the magnetic separation as a new way for separation of organocatalysts. However, in many examples, magnetic NPs (such as Fe₃O₄ and γ-Fe₂O₃) can catalyze a number of organic reactions due to its Lewis acid nature, besides the function as a magnetic core^{179,180}.

Mechanical force could be employed as a stimulus for catalysis¹⁸¹. Generally, mechanical forces are applied in solution through the use of ultrasound¹⁸², and in solid state via collisions using milling balls¹⁸³. However, reversible control over catalytic activity in aqueous environments using this stimulus is scarce. Deactivation of catalytic species by generated radical during sonication and the requirement of large macromolecular chain that can be affected during sonication are the major limitations of using this stimulus for control catalytic activity. In addition, water can be only employed in liquid assisted grinding technique of milling ball approach¹⁸⁴, but the process is not reversible. Nonetheless, more detailed insights for the mechanisms and processes underlying mechanochemical catalyst (de)activation can contribute to the rational design and implementation of switchable mechanocatalyzed systems in aqueous environments, with their potential use in smart application¹⁸⁵.

Conclusion and outlook

In conclusion, this account summarizes the advances in switchable catalytic systems in aqueous medium. Various “nature-like” catalyst systems including supramolecular aggregations, nanoreactors,

and molecular catalysts have been enlisted. Taking inspiration from enzymatic activity in aqueous environments, reversible control over artificial catalytic systems for organic transformations has been challenging. However, significant advances have been made in the field of switchable aqueous catalytic systems either via improved catalyst design or via creation of a favorable microenvironment for the catalysis. The later approach is very similar in analogy to the natural enzyme, where hydrophobic pockets provide the optimal chemical environment. Artificial switchable catalysts can alter the reaction rate, selectivity in aqueous environments, but only a handful of organic transformations are successfully tested as benchmark reactions. Limited solubility of the substances and stability of the reaction intermediates are the typical drawbacks for “in water” organic transformations, whereas “on water” reactions can be performed for hydrophobic substances¹⁵. However, more strategies for creation of favorable active-site microenvironment via catalysis engineering should be developed, where both hydrophilic and hydrophobic substances can undergo synthetic transformations in aqueous environment, and the catalysis can be switched “on” and “off” in presence/absence of stimuli. Besides, most efforts are concentrated on the invention of new types of switchable catalyst systems incorporating stimuli-responsive unit within their architecture for controlling over the catalytic activity. Moreover, majority of the catalytic systems have modest differences between the catalytic activities of ‘on’ and ‘off’ states of the systems. Although the field is in its infancy, artificial aqueous catalyst system requires development in the catalytic systems that accelerate the rate of reaction in the ‘on’ state and no reaction in the ‘off’ state. Besides, new chemical transformations with wider substrate scope should be tested.

Engineering over aqueous organocatalysis can be expected to grow in the coming years with a further broadening of its applications in biological environments. Besides stimuli-induced control over reaction rate, other characteristics such as substrate/product-selectivity have to be studied in switchable organocatalysis. It is worth noting that each stimulus comes with its own advantages and disadvantages for catalytic systems. As stimulus, temperature is employed mostly for switchable catalytic systems. These systems comprise PNIPAm or other polymers with different transition temperatures, whose efficiency can be switched in a wide range of temperatures. However, degradation at high temperature and probability of having side products are the limitation for temperature stimulus. Light has been used as noninvasive external trigger, which allows control in spatio-temporal precision. However, most of the examples are based on azobenzene-based molecules, while a larger variability could be obtained by employing different photoswitchable compounds. Electrochemically induced redox-switchable systems are convenient for metal-based catalysts due to easy modulation of redox-potential of the metal center. However, limitations regarding electrodes, and electrolytes remain major challenges in this field. With ongoing technological advancement, the scope, utility, and versatility of various stimuli-induced aqueous catalysis for organic transformations will continue to grow¹⁸⁶. Altogether, a bright future is ahead for smart organocatalytic processes and encourage their applications in biological systems.

Received: 4 July 2022; Accepted: 12 September 2022;
Published online: 26 September 2022

References

1. Motlagh, H. N., Wrabl, J. O., Li, J. & Hilser, V. J. The ensemble nature of allostery. *Nature* **508**, 331–339 (2014).

2. Dong, Z., Luo, Q. & Liu, J. Artificial enzymes based on supramolecular scaffolds. *Chem. Soc. Rev.* **41**, 7890–7908 (2012). **This article provides an overview of artificial enzymes based on supramolecular scaffolds.**
3. Raynal, M., Ballester, P., Vidal-Ferran, A. & van Leeuwen, P. W. Supramolecular catalysis. Part 2: artificial enzyme mimics. *Chem. Soc. Rev.* **43**, 1734–1785 (2014).
4. Eelkema, R. & van Esch, J. H. Catalytic control over the formation of supramolecular materials. *Org. Biomol. Chem.* **12**, 6292–6296 (2014).
5. Maity, C., Trausel, F. & Eelkema, R. Selective activation of organocatalysts by specific signals. *Chem. Sci.* **9**, 5999–6005 (2018).
6. Guruge, C. et al. Caged proline in photoinitiated organocatalysis. *J. Org. Chem.* **84**, 5236–5244 (2019).
7. Blanco, V., Leigh, D. A. & Marcos, V. Artificial switchable catalysts. *Chem. Soc. Rev.* **44**, 5341–5370 (2015). **The article reviews switchable catalytic systems whose activity and/or selectivity can be controlled by stimuli.**
8. Choudhury, J. Recent developments on artificial switchable catalysis. *Tetrahedron Lett.* **59**, 487–495 (2018).
9. Hazra, S., Gallou, F. & Handa, S. Water: an underestimated solvent for amide bond-forming reactions. *ACS Sustain. Chem. Eng.* **10**, 5299–5306 (2022).
10. Lipshutz, B. L. When does organic chemistry follow nature’s lead and “make the switch”? *J. Org. Chem.* **82**, 2806–2816 (2017).
11. Jimeno, C. Water in asymmetric organocatalytic systems: a global perspective. *Org. Biomol. Chem.* **14**, 6147–6164 (2016).
12. Kitanosono, T., Masuda, K., Xu, P. & Kobayashi, S. Catalytic organic reactions in water toward sustainable society. *Chem. Rev.* **118**, 679–746 (2018).
13. Blackmond, D. G., Armstrong, A., Coombe, V. & Wells, A. Water in organocatalytic processes: debunking the myths. *Angew. Chem. Int. Ed.* **46**, 3798–3800 (2007).
14. Raj, M. & Singh, V. K. Organocatalytic reactions in water. *Chem. Commun.* 6687–6703, <https://doi.org/10.1039/b910861k> (2009).
15. Cortes-Clerget, M. et al. Water as the reaction medium in organic chemistry: from our worst enemy to our best friend. *Chem. Sci.* **12**, 4237–4266 (2021). **This article provides a discussion about water as medium for organic reactions including “on water” and “in water” phenomena.**
16. Serrano-Luginbühl, S., Ruiz-Mirazo, K., Ostaszewski, R., Gallou, F. & Walde, P. Soft and dispersed interface-rich aqueous systems that promote and guide chemical reactions. *Nat. Rev. Chem.* **2**, 306–327 (2018).
17. Butler, R. N. & Coyne, A. G. Water: Nature’s reaction enforcer-comparative effects for organic synthesis “In-water” and “On-water”. *Chem. Rev.* **110**, 6302–6337 (2010).
18. Brogan, A. P., Dickerson, T. J. & Janda, K. D. Enamine-based aldol organocatalysis in water: are they really “All Wet”? *Angew. Chem. Int. Ed.* **45**, 8100–8102 (2006).
19. Mase, N. & Barbas, C. F. III In water, on water, and by water: mimicking nature’s aldolases with organocatalysis and water. *Org. Biomol. Chem.* **8**, 4043–4050 (2010).
20. Kitanosono, T. & Kobayashi, S. Reactions in water through “On-Water” mechanism. *Chem. Eur. J.* **26**, 9408–9429 (2020).
21. Liu, S., Du, P., Sun, H., Yu, H.-Y. & Wang, Z.-G. Bioinspired supramolecular catalysts from designed self-assembly of DNA or peptides. *ACS Catal.* **10**, 14937–14958 (2020).
22. van der Helm, M. P., Klemm, B. & Eelkema, R. Organocatalysis in aqueous media. *Nat. Rev. Chem.* **3**, 491–508 (2019). **The article provides a comprehensive overview of organocatalytic reactions in aqueous media including reaction mechanism and comparison with enzymatic activity.**
23. Ostermeier, M. Designing switchable enzymes. *Curr. Opin. Struct. Biol.* **19**, 442–448 (2009).
24. Winkler, C. K., Schrittwieser, J. H. & Kroutil, W. Power of biocatalysis for organic synthesis. *ACS Cent. Sci.* **7**, 55–71 (2021).
25. Wells, P. K., Smutok, O., Melman, A. & Katz, E. Switchable biocatalytic reactions controlled by interfacial pH changes produced by orthogonal biocatalytic processes. *ACS Appl. Mater. Interfaces* **13**, 33830–33839 (2021).
26. Fastrez, J. Engineering allosteric regulation into biological catalysts. *ChemBiochem* **10**, 2824–2835 (2009).
27. Callender, R. & Dyer, R. B. Advances in time-resolved approaches to characterize the dynamical nature of enzymatic catalysis. *Chem. Rev.* **106**, 3031–3042 (2006).
28. Makhlynets, O. V., Raymond, E. A. & Korendovych, I. V. Design of allosterically regulated protein catalysts. *Biochemistry* **54**, 1444–1445 (2015).
29. Solomon, L. A., Kronenberg, J. B. & Fry, H. C. Control of heme coordination and catalytic activity by conformational changes in peptide-amphiphile assemblies. *J. Am. Chem. Soc.* **139**, 8497–8507 (2017).
30. Plaut, B. & Knowles, J. R. pH-dependence of the triose phosphate isomerase reaction. *Biochem. J.* **129**, 311–320 (1972).
31. Raines, R. T., Sutton, E. L., Straus, D. R., Gilbert, W. & Knowles, J. R. Reaction energetics of a mutant triose phosphate isomerase in which the active-site glutamate has been changed to aspartate. *Biochemistry* **25**, 7142–7154 (1986).
32. Lodi, P. J. & Knowles, J. R. Neutral imidazole is the electrophile in the reaction catalyzed by triosephosphate isomerase: structural origins and catalytic implications. *Biochemistry* **30**, 6948–6956 (1991).
33. Guler, M. O. & Stupp, S. I. A self-assembled nanofiber catalyst for ester hydrolysis. *J. Am. Chem. Soc.* **129**, 12082–12083 (2007).
34. Zhang, C. et al. Self-assembled peptide nanofibers designed as biological enzymes for catalyzing ester hydrolysis. *ACS Nano* **8**, 11715–11723 (2014).
35. Huerta, E. et al. Triggering activity of catalytic rod-like supramolecular polymers. *Chem. Eur. J.* **21**, 3682–3690 (2015).
36. Bohmwick, S., Zhang, L., Ouyang, G. & Liu, M. Self-assembly of amphiphilic dipeptide with homo- and heterochiral centers and their application in asymmetric aldol reaction. *ACS Omega* **3**, 8329–8336 (2018).
37. Arlegui, A. et al. Spontaneous mirror-symmetry breaking coupled to top-bottom chirality transfer: from porphyrin self-assembly to scalemic Diels–Alder adducts. *Chem. Commun.* **55**, 12219–12222 (2019).
38. Che, H. & van Hest, J. C. M. Adaptive polymersome nanoreactors. *ChemNanoMat* **5**, 1092–1109 (2019).
39. Zhang, C. et al. Switchable hydrolase based on reversible formation of supramolecular catalytic site using a self-assembling peptide. *Angew. Chem. Int. Ed.* **56**, 14511–14515 (2017).
40. Arlegui, A., Torres, P., Cuesta, V., Crusats, J. & Moyano, A. A pH-switchable aqueous organocatalysis with amphiphilic secondary amine–porphyrin hybrids. *Eur. J. Org. Chem.* **2020**, 4399–4407 (2020).
41. Kocak, G., Tuncer, C. & Bütün, V. pH-Responsive polymers. *Polym. Chem.* **8**, 144–176 (2017).
42. Altava, B., Burguete, M. I., García-Verdugo, E. & Luis, S. V. Chiral catalysts immobilized on achiral polymers: effect of the polymer support on the performance of the catalyst. *Chem. Soc. Rev.* **47**, 2722–2771 (2018).
43. List, B. Proline-catalyzed asymmetric reactions. *Tetrahedron* **58**, 5573–5590 (2002).
44. Gruttadauria, M., Giacalone, F. & Noto, R. Supported proline and proline-derivatives as recyclable organocatalysts. *Chem. Soc. Rev.* **37**, 1666–1688 (2008).
45. Sakthivel, K., Notz, W., Bui, T. & Barbas, C. F. Amino acid catalyzed direct asymmetric aldol reactions: a bioorganic approach to catalytic asymmetric carbon–carbon bond-forming reactions. *J. Am. Chem. Soc.* **123**, 5260–5267 (2001).
46. Hayashi, Y. In water or in the presence of water? *Angew. Chem. Int. Ed.* **45**, 8103–8104 (2006).
47. Lipshutz, B. H. & Ghorai, S. Organocatalysis in water at room temperature with in-flask catalyst recycling. *Org. Lett.* **14**, 422–425 (2012).
48. van Oers, M. C. M., Veldmate, W. S., van Hest, J. C. M. & Rutjes, F. P. J. T. Aqueous asymmetric aldol reactions in polymersome membranes. *Polym. Chem.* **6**, 5358–5361 (2015).
49. Doyagüez, E. G. et al. Linear copolymers of proline methacrylate and styrene as catalysts for aldol reactions in water: Effect of the copolymer aggregation on the enantioselectivity. *Macromolecules* **44**, 6268–6276 (2011).
50. Prado, A. D. et al. Aqueous micro and nanoreactors based on alternating copolymers of phenylmaleimide and vinylpyrrolidone bearing pendant L-proline stabilized with PEG grafted chain. *J. Polym. Sci. A Polym. Chem.* **55**, 1228–1236 (2016).
51. Tang, Y. et al. L-Proline functionalized pH-responsive copolymers as supported organocatalysts for asymmetric aldol reaction in water. *React. Funct. Polym.* **150**, 104544 (2020).
52. Zotova, N., Franke, A., Armstrong, A. & Blackmond, D. G. Clarification of the role of water in proline-mediated aldol reactions. *J. Am. Chem. Soc.* **129**, 15100–15101 (2007).
53. Thomas, J. M. & Thomas, W. J. *Principles and Practice of Heterogeneous Catalysis* (Wiley-VCH, Weinheim, 1997).
54. Chng, L. L., Erathodiyil, N. & Ying, J. Y. Nanostructured catalysts for organic transformations. *Acc. Chem. Res.* **46**, 1825–1837 (2013). **This article reviews the use of nanostructured materials for catalytic organic reactions.**
55. Chiozzi, V. & Rossi, F. Inorganic–organic core/shell nanoparticles: progress and applications. *Nanoscale Adv.* **2**, 5090–5105 (2020).
56. Zhang, M. & Zhang, W. Pd nanoparticles immobilized on pH-responsive and chelating nanospheres as an efficient and recyclable catalyst for Suzuki reaction in water. *J. Phys. Chem. C* **112**, 6245–6252 (2008).
57. Xiao, C., Chen, S., Zhang, L., Zhou, S. & Wu, W. One-pot synthesis of responsive catalytic Au@PVP hybrid nanogels. *Chem. Commun.* **48**, 11751–11753 (2012).
58. Ansari, S. N., Chakraborty, S. & Kitchens, C. L. pH-Responsive mercaptoundecanoic acid functionalized gold nanoparticles and applications in catalysis. *Nanomaterials* **8**, 339 (2018).
59. Ni, L., Yu, C., Wei, Q., Liu, D. & Qiu, J. Pickering emulsion catalysis: Interfacial chemistry, catalyst design, challenges, and perspectives. *Angew. Chem. Int. Ed.* **61**, e202115885 (2022).
60. Yang, Y. et al. An Overview of pickering emulsions: solid-particle materials, classification, morphology, and applications. *Front. Pharmacol.* **8**, 287 (2017).

61. Chang, F., Vis, C. M., Ciptonugroho, W. & Bruijninx, P. C. A. Recent developments in catalysis with pickering emulsions. *Green Chem.* **23**, 2575–2594 (2021). **The article provides an overview of Pickering emulsions catalysis.**
62. Yang, H., Zhou, T. & Zhang, W. A strategy for separating and recycling solid catalysts based on the pH-triggered pickering-emulsion inversion. *Angew. Chem. Int. Ed.* **52**, 7455–7459 (2013).
63. Fang, Z., Yang, D., Gao, Y. & Li, H. pH-Responsible pickering emulsion and its catalytic application for reaction at water–oil interface. *Colloid Polym. Sci.* **293**, 1505–1513 (2015).
64. Qi, L., Luo, Z. & Lu, X. Facile synthesis of starch-based nanoparticles stabilized pickering emulsion: its pH-responsive behavior and application for the recyclable catalysis. *Green Chem.* **20**, 1538–1550 (2018).
65. Arcus, V. L. et al. On the temperature dependence of enzyme-catalyzed rates. *Biochemistry* **55**, 1681–1688 (2016).
66. Frazar, E. M., Shah, R. A., Dziubla, T. D. & Hilt, J. Z. Multifunctional temperature-responsive polymers as advanced biomaterials and beyond. *J. Appl. Polym. Sci.* **137**, 48770 (2019).
67. Liu, H., Prachyathipsakul, T., Koyasser-Yehiya, T. M., Le, S. P. & Thayumanavan, S. Molecular bases for temperature sensitivity in supramolecular assemblies and their applications as thermoresponsive soft materials. *Mater. Horiz.* **9**, 164–193 (2022).
68. Zhang, J., Zhang, M., Tang, K., Verpoort, F. & Sun, T. Polymer-based stimuli-responsive recyclable catalytic systems for organic synthesis. *Small* **10**, 32–46 (2014).
69. Wei, W., Zhu, M., Wu, S., Shen, X. & Li, S. Stimuli-responsive biopolymers: an inspiration for synthetic smart materials and their applications in self-controlled catalysis. *J. Inorg. Organomet. Polym.* **30**, 69–87 (2020).
70. Gaitsch, J., Huang, X. & Voit, B. Engineering functional polymer capsules toward smart nanoreactors. *Chem. Rev.* **116**, 1053–1093 (2016).
71. Shen, T. et al. Recent advances on micellar catalysis in water. *Adv. Colloid Interface Sci.* **287**, 102299 (2021).
72. Zayas, H. A. et al. Thermoresponsive polymer-supported L-proline micelle catalysts for the direct asymmetric aldol reaction in water. *ACS Macro Lett.* **2**, 327–331 (2013).
73. Ge, Z. et al. Stimuli-responsive double hydrophilic block copolymer micelles with switchable catalytic activity. *Macromolecules* **40**, 3538–3546 (2007).
74. Yu, X., Herberg, A. & Kuckling, D. Micellar organocatalysis using smart polymer supports: influence of thermoresponsive self-assembly on catalytic activity. *Polymers* **12**, 2265 (2020).
75. Plamper, F. A. & Richtering, W. Functional microgels and microgel systems. *Acc. Chem. Res.* **50**, 131–140 (2017).
76. Tan, K. H. et al. Selenium-modified microgels as bio-inspired oxidation catalysts. *Angew. Chem. Int. Ed.* **58**, 9791–9796 (2019).
77. Lu, A., Cotanda, P., Patterson, J. P., Longbottom, D. A. & O'Reilly, R. K. Aldol reactions catalyzed by L-proline functionalized polymeric nanoreactors in water. *Chem. Commun.* **48**, 9699–9701 (2012).
78. Chen, T. et al. Highly efficient polymer-based nanoreactors for selective oxidation of alcohols in water. *Mol. Catal.* **474**, 110422 (2019).
79. Chen, T. et al. Triphenylphosphine-containing thermo-responsive copolymers: synthesis, characterization and catalysis application. *Macromol. Res.* **27**, 931–937 (2019).
80. Kuepfert, M., Ahmed, E. & Weck, M. Self-assembled thermoresponsive molecular brushes as nanoreactors for asymmetric aldol addition in water. *Macromolecules* **54**, 3845–3853 (2021).
81. Cotanda, P., Lu, A., Patterson, J. P., Petzetakis, N. & O'Reilly, R. K. Functionalized organocatalytic nanoreactors: hydrophobic pockets for acylation reactions in water. *Macromolecules* **45**, 2377 (2012).
82. He, X. et al. Synthetic homeostatic materials with chemo-mechano-chemical self-regulation. *Nature* **487**, 214–218 (2012). **This article provides an example of catalyst engineering for controlled chemical conversion via control over local environment.**
83. Zarzar, L. D. & Aizenberg, J. Stimuli-responsive chemomechanical actuation: a hybrid materials approach. *Acc. Chem. Res.* **47**, 530–539 (2014).
84. Lu, A., Moatsou, D., Hands-Portman, I., Longbottom, D. A. & O'Reilly, R. K. Recyclable L-proline functional nanoreactors with temperature-tuned activity based on core–shell nanogels. *ACS Macro Lett.* **3**, 1235–1239 (2014).
85. Lu, Y., Mei, Y., Drechsler, M. & Ballauff, M. Thermosensitive core-shell particles as carriers for Ag nanoparticles: modulating the catalytic activity by a phase transition in networks. *Angew. Chem. Int. Ed.* **45**, 813–816 (2006).
86. Lu, Y. et al. Thermosensitive core-shell microgel as a “nanoreactor” for catalytic active metal nanoparticles. *J. Mater. Chem.* **19**, 3955 (2009).
87. Wang, Y., Yan, R., Zhang, J. & Zhang, W. Synthesis of efficient and reusable catalyst of size-controlled Au nanoparticles within a porous, chelating and intelligent hydrogel for aerobic alcohol oxidation. *J. Mol. Catal. A: Chem.* **317**, 81–88 (2010).
88. Xiong, D. et al. Modulating the catalytic activity of Au/micelles by tunable hydrophilic channels. *J. Colloid Interface Sci.* **341**, 273–279 (2010).
89. Huang, X. et al. Smart microgel catalyst with modulatory glutathione peroxidase activity. *Soft Matter* **5**, 1905–1911 (2009).
90. Boucher-Jacobs, C., Rabnawaz, M., Katz, J. S., Even, R. & Guirounet, D. Encapsulation of catalyst in block copolymer micelles for the polymerization of ethylene in aqueous medium. *Nat. Commun.* **9**, 841 (2018).
91. Tevet, S., Wagle, S. S., Slor, G. & Amir, R. J. Tuning the reactivity of micellar nanoreactors by precise adjustments of the amphiphile and substrate hydrophobicity. *Macromolecules* **54**, 11419–11426 (2021).
92. Pang, H., Hu, Y., Yu, J., Gallou, F. & Lipshutz, B. H. Water-sculpting of a heterogeneous nanoparticle precatalyst for Mizoroki–Heck couplings under aqueous micellar catalysis conditions. *J. Am. Chem. Soc.* **143**, 3373–3382 (2021).
93. Xiao, X. C., Chu, L. Y., Chen, W. M., Wang, S. & Li, Y. Positively thermo-sensitive monodisperse core-shell microspheres. *Adv. Funct. Mater.* **13**, 847–852 (2003).
94. Li, S., Ge, Y., Tiwari, A. & Cao, S. A temperature-responsive nanoreactor. *Small* **6**, 2453–2459 (2010).
95. Tian, J., Huang, B. & Zhang, W. Precise self-assembly and controlled catalysis of thermoresponsive core-satellite multicomponent hybrid nanoparticles. *Langmuir* **35**, 266–275 (2019).
96. O'Reilly, R. K., Hawker, C. J. & Wooley, K. L. Cross-linked block copolymer micelles: functional nanostructures of great potential and versatility. *Chem. Soc. Rev.* **35**, 1068 (2006).
97. Dong, Y. et al. Thermo-responsive polymer-tethered and Pd NPs loaded UiO-66 NMOF for biphasic CBs dechlorination. *Green Chem.* **21**, 1625–1634 (2019).
98. Winarta, J. et al. A decade of UiO-66 research: a historic review of dynamic structure, synthesis mechanisms, and characterization techniques of an archetypal metal-organic framework. *Cryst. Growth Des.* **20**, 1347–1362 (2020).
99. Rizzo, C., Marullo, S., Billeci, F. & D'Anna, F. Catalysis in supramolecular systems: the case of gel phases. *Eur. J. Org. Chem.* **22**, 3148–3169 (2021).
100. Foster, J. A. & Steed, J. W. Exploiting cavities in supramolecular gels. *Angew. Chem. Int. Ed.* **49**, 6718–6724 (2010).
101. Neumann, L. N. et al. Supramolecular polymers for organocatalysis in water. *Org. Biomol. Chem.* **13**, 7711 (2015).
102. Díaz Díaz, D., Kühbeck, D. & Koopmans, R. J. Stimuli-responsive gels as reaction vessels and reusable catalysts. *Chem. Soc. Rev.* **40**, 427 (2011).
103. Hapiot, F., Menuel, S. & Monflier, E. Thermoresponsive hydrogels in catalysis. *ACS Catal.* **3**, 1006–1010 (2013).
104. Rodríguez-Llansola, F., Escuder, B. & Miravet, J. F. Switchable performance of an L-proline-derived basic catalyst controlled by supramolecular gelation. *J. Am. Chem. Soc.* **131**, 11478–11484 (2009).
105. Léger, B., Menuel, S., Ponchel, A., Hapiot, F. & Monflier, E. Nanoparticle-based catalysis using supramolecular hydrogels. *Adv. Synth. Catal.* **354**, 1269–1272 (2012).
106. Durr, H. & Bouas-Laurent, H. *Photochromism: Molecules and Systems* (Elsevier, 2003). **This book gives a comprehensive review of photochromic molecules and photoresponsive systems.**
107. Neilson, B. M. & Bielawski, C. W. Illuminating photoswitchable catalysis. *ACS Catal.* **3**, 1874–1885 (2013).
108. Vlatkovic, M., Collins, B. S. L. & Feringa, B. L. Dynamic responsive systems for catalytic function. *Chem. Eur. J.* **22**, 17080–17111 (2016).
109. van Dijk, L. et al. Molecular machines for catalysis. *Nat. Rev. Chem.* **2**, 0117 (2018). **This article provides a comprehensive overview of molecular machines as catalysts for controlling chemical reactions.**
110. Stoll, R. S. & Hecht, S. Artificial light-gated catalyst systems. *Angew. Chem. Int. Ed.* **49**, 5054–5075 (2010).
111. Toney, M. D. Controlling reaction specificity in pyridoxal phosphate enzymes. *Biochim. Biophys. Acta* **1814**, 1407–1418 (2011).
112. Wilson, D. & Branda, N. R. Turning “On” and “Off” a pyridoxal 5'-phosphate mimic using light. *Angew. Chem. Int. Ed.* **51**, 5431–5434 (2012).
113. Ueno, A., Takahashi, K. & Osa, T. Photoregulation of catalytic activity of β -cyclodextrin by an azo inhibitor. *J. Chem. Soc., Chem. Commun.* 837–838, <https://doi.org/10.1039/C39800000837> (1980).
114. Ueno, A., Takahashi, K. & Osa, T. Photocontrol of catalytic activity of capped cyclodextrin. *J. Chem. Soc., Chem. Commun.* **3**, 94–96 (1981).
115. Lee, W.-S. & Ueno, A. Photocontrol of the catalytic activity of a β -cyclodextrin bearing azobenzene and histidine moieties as a pendant group. *Macromol. Rapid Commun.* **22**, 448–450 (2001).
116. Zhu, L. et al. Photoswitchable supramolecular catalysis by interparticle host-guest competitive binding. *Chem. Eur. J.* **18**, 13979–13983 (2012).
117. Zhao, Y. et al. A supramolecular approach to construct a hydrolase mimic with photo-switchable catalytic activity. *J. Mater. Chem. B* **6**, 2444–2449 (2018).
118. Imahori, T. & Kurihara, S. Stimuli-responsive cooperative catalysts based on dynamic conformational changes toward spatiotemporal control of chemical reactions. *Chem. Lett.* **43**, 1524–1531 (2014).

119. Samanta, M., Ramakrishna, V. S. & Bandyopadhyay, S. A photoresponsive glycosidase mimic. *Chem. Commun.* **50**, 10577–10579 (2014).
120. Zechel, D. L. & Withers, S. G. Glycosidase mechanisms: anatomy of a finely tuned catalyst. *Acc. Chem. Res.* **33**, 11–18 (2000).
121. Kim, C. U. et al. Tracking solvent and protein movement during CO₂ release in carbonic anhydrase II crystals. *Proc. Natl Acad. Sci. USA* **113**, 5257–5262 (2016).
122. Saha, M. & Bandyopadhyay, S. A reversible photoresponsive activity of a carbonic anhydrase mimic. *Chem. Commun.* **55**, 3294–3297 (2019).
123. Ren, C. Z.-J., Muñana, P. S., Dupont, J., Zhou, S. S. & Chen, J. L.-Y. Reversible formation of a light-responsive catalyst by utilizing intermolecular cooperative effects. *Angew. Chem. Int. Ed.* **58**, 15254 (2019).
124. Neri, S., Martin, S. G., Pezzato, C. & Prins, L. J. Photoswitchable catalysis by a nanozyme mediated by a light-sensitive cofactor. *J. Am. Chem. Soc.* **139**, 1794–1797 (2017).
125. Sanchez-Iglesias, A. et al. Hydrophobic interactions modulate self-assembly of nanoparticles. *ACS Nano* **6**, 11059–11065 (2012).
126. Kundu, P., Olsen, G., Kiss, V. & Klajn, R. Nanoporous frameworks exhibiting multiple stimuli responsiveness. *Nat. Commun.* **5**, 3588 (2014).
127. Zhao, H. et al. Reversible trapping and reaction acceleration within dynamically self-assembling nanoflasks. *Nat. Nanotech.* **11**, 82–88 (2016).
This article is an example of catalysis engineering for controlled chemical reaction employing light as stimulus.
128. Li, Z. et al. Light-switched reversible emulsification and demulsification of oil-in-water Pickering emulsions. *Angew. Chem. Int. Ed.* **60**, 3928–3933 (2021).
129. Niu, F., Zhai, J., Jiang, L. & Song, W.-G. Light induced activity switch in interfacial hydrogen-bond catalysis with photo sensitive metal oxides. *Chem. Commun.* **31**, 4738–4740 (2009).
130. Kawasaki, H. et al. Reversible vesicle formation by changing pH. *J. Phys. Chem. B* **106**, 1524–1527 (2002).
131. Dwars, T., Paetzold, E. & Oehme, G. Reactions in micellar systems. *Angew. Chem. Int. Ed.* **44**, 7174–7199 (2005).
132. Sinibaldi, A. et al. Asymmetric organocatalysis accelerated via self-assembled minimal structures. *Eur. J. Org. Chem.* **39**, 5403–5406 (2021).
133. Zhang, B. et al. The synthesis of chiral isotretinonic acids with amphiphilic imidazole/pyrrolidine catalysts assembled in oil-in-water emulsion droplets. *Angew. Chem. Int. Ed.* **51**, 13159–13162 (2012).
134. Qin, L. et al. Supramolecular assemblies of amphiphilic L-proline regulated by compressed CO₂ as a recyclable organocatalyst for the asymmetric aldol reaction. *Angew. Chem. Int. Ed.* **52**, 7761–7765 (2013).
135. Yoon, H. J., Kuwabara, J., Kim, J.-H. & Mirkin, C. A. Allosteric supramolecular triple-layer catalysts. *Science* **330**, 66–69 (2010).
136. Lifschitz, A. M. et al. An allosteric photoredox catalyst inspired by photosynthetic machinery. *Nat. Commun.* **6**, 6541 (2015).
137. Goswami, A., Saha, S., Biswas, P. K. & Schmittel, M. Nano(mechanical) motion triggered by metal coordination: from functional devices to networked multicomponent catalytic machinery. *Chem. Rev.* **120**, 125–199 (2020).
138. Kovbasyuk, L. & Krämer, R. Allosteric supramolecular receptors and catalysts. *Chem. Rev.* **104**, 3161–3187 (2004).
139. Pan, T., Wang, Y., Xue, X. & Zhang, C. Rational design of allosteric switchable catalysts. *Exploration* **2**, 20210095 (2022).
140. Yoon, H. J., Heo, J. & Mirkin, C. A. Allosteric regulation of phosphate diester transesterification based upon a dinuclear zinc catalyst assembled via the weak-link approach. *J. Am. Chem. Soc.* **129**, 14182–14183 (2007).
141. Farrell, J. R., Mirkin, C. A., Guzei, I. A., Liable-Sands, L. M. & Rheingold, A. L. The weak-link approach to the synthesis of inorganic macrocycles. *Angew. Chem. Int. Ed.* **37**, 465–467 (1998).
142. Allen, A. E. & MacMillan, D. W. C. Synergistic catalysis: a powerful synthetic strategy for new reaction development. *Chem. Sci.* **3**, 633–658 (2012).
143. Pimentel, E. B., Peters-Clarke, T. M., Coon, J. J. & Martell, J. D. DNA-scaffolded synergistic catalysis. *J. Am. Chem. Soc.* **143**, 21402–21409 (2021).
144. Comellas-Aragonès, M. et al. A virus-based single-enzyme nanoreactor. *Nat. Nanotech.* **2**, 635–639 (2007).
145. Buddingh, B. C. & van Hest, J. C. M. Artificial cells: synthetic compartments with life-like functionality and adaptivity. *Acc. Chem. Res.* **50**, 769–777 (2017).
146. Vázquez-González, M., Wang, C. & Willner, I. Biocatalytic cascades operating on macromolecular scaffolds and in confined environments. *Nat. Catal.* **3**, 256–273 (2020).
147. Liu, S. et al. DNA nanotweezers for biosensing applications: Recent advances and future prospects. *ACS Sens.* **7**, 3–20 (2022).
148. Watson, E. E., Angerani, S., Sabale, P. M. & Winssinger, N. Biosupramolecular systems: integrating cues into responses. *J. Am. Chem. Soc.* **143**, 4467–4482 (2021).
149. Mukherjee, P., Leman, L. J., Griffin, J. H. & Ghadiri, M. R. Design of a DNA-programmed plasminogen activator. *J. Am. Chem. Soc.* **140**, 15516–15524 (2018).
150. Boekhoven, J., Hendriksen, W. E., Koper, G. J. M., Eelkema, R. & van Esch, J. H. Transient assembly of active materials fueled by a chemical reaction. *Science* **349**, 1075–1079 (2015).
151. van Rossum, S. A. P., Tena-Solsona, M., van Esch, J. H., Eelkema, R. & Boekhoven, J. Dissipative out-of-equilibrium assembly of man-made supramolecular materials. *Chem. Soc. Rev.* **46**, 5519–5535 (2017).
152. Grzybowski, B. A. & Huck, W. T. S. The nanotechnology of life-inspired systems. *Nat. Nanotechnol.* **11**, 585–592 (2016).
153. Singh, N., Formon, G. J. M., De Piccoli, S. & Hermans, T. M. Devising synthetic reaction cycles for dissipative nonequilibrium self-assembly. *Adv. Mater.* **32**, 1906834 (2020).
154. Das, K., Gabrielli, L. & Prins, L. J. Chemically-fueled self-assembly in biology and chemistry. *Angew. Chem. Int. Ed.* **60**, 20120–20143 (2021).
155. Kathan, M. & Hecht, S. Photoswitchable molecules as key ingredients to drive systems away from the global thermodynamic minimum. *Chem. Soc. Rev.* **46**, 5536–5550 (2017).
156. van Leeuwen, T., Lubbe, A. S., Štacko, P., Wezenberg, S. J. & Feringa, B. L. Dynamic control of function by light-driven molecular motors. *Nat. Rev. Chem.* **1**, 0096 (2017).
157. Amano, S., Borsley, S., Leigh, D. A. & Zhanhu, S. Chemical engines: driving systems away from equilibrium through catalyst reaction cycles. *Nat. Nanotechnol.* **16**, 1057–1067 (2021).
158. Maiti, S., Fortunati, I., Ferrante, C., Scrimin, P. & Prins, L. J. Dissipative self-assembly of vesicular nanoreactors. *Nat. Chem.* **8**, 725–731 (2016).
159. Cardona, M. A. & Prins, L. J. ATP-fuelled self-assembly to regulate chemical reactivity in the time domain. *Chem. Sci.* **11**, 1518–1522 (2020).
160. Zhang, L., Marcos, V. & Leigh, D. A. Molecular machines with bio-inspired mechanisms. *Proc. Natl Acad. Sci. USA* **115**, 9397–9404 (2018).
161. Wilson, M. R. et al. An autonomous chemically fuelled small-molecule motor. *Nature* **534**, 235–240 (2016).
162. Heard, A. W., Suárez, J. M. & Goldup, S. M. Controlling catalyst activity, chemoselectivity and stereoselectivity with the mechanical bond. *Nat. Rev. Chem.* **6**, 182–196 (2022). **This article provides an overview of mechanically interlocked molecules for catalytic applications.**
163. Muñana, S. P. et al. Substrate-induced self-assembly of cooperative catalysts. *Angew. Chem. Int. Ed.* **57**, 16469–16474 (2018).
164. Biagini, C. et al. Dissipative catalysis with a molecular machine. *Angew. Chem. Int. Ed.* **58**, 9876 (2019).
165. van der Helm, M. P., Li, G., Hartono, M. & Eelkema, R. Transient host–guest complexation to control catalytic activity. *J. Am. Chem. Soc.* **144**, 9465 (2022).
166. Möhle, S. et al. Modern electrochemical aspects for the synthesis of value-added organic products. *Angew. Chem. Int. Ed.* **57**, 6018 (2018).
167. Siu, J. C., Fu, N. & Lin, S. Catalyzing electrosynthesis: a homogeneous electrocatalytic approach to reaction discovery. *Acc. Chem. Res.* **53**, 547–560 (2020).
168. Giljohann, D. A. et al. Gold nanoparticles for biology and medicine. *Angew. Chem. Int. Ed.* **49**, 3280–3294 (2010).
169. Prins, L. J. Emergence of complex chemistry on an organic monolayer. *Acc. Chem. Res.* **48**, 1920–1928 (2015).
170. della Sala, F. et al. Reversible electrochemical modulation of a catalytic nanosystem. *Angew. Chem. Int. Ed.* **55**, 10737 (2016).
171. Qu, Y., Sun, D. & Yu, Y. Interfacial engineering in pickering emulsion photocatalytic microreactors: from mechanisms to prospects. *Chem. Eng. J.* **438**, 135655 (2022).
172. Shi, Y. et al. Ambient CO₂/N₂ switchable pickering emulsion emulsified by TETA-functionalized metal–organic frameworks. *ACS Appl. Mater. Interfaces* **12**, 53385–53393 (2020).
173. Byun, J., Huang, W., Wang, D., Li, R. & Zhang, K. A. I. CO₂-triggered switchable hydrophilicity of heterogeneous conjugated polymer photocatalyst for enhanced catalytic activity in water. *Angew. Chem. Int. Ed.* **57**, 2967–2971 (2018).
174. Cheng, T., Zhang, D., Lia, H. & Liu, G. Magnetically recoverable nanoparticles as efficient catalysts for organic transformations in aqueous medium. *Green. Chem.* **16**, 3401–3427 (2014).
175. Mrówczyński, R., Nan, A. & Liebscher, J. Magnetic nanoparticle-supported organocatalysts—an efficient way of recycling and reuse. *RSC Adv.* **4**, 5927–5952 (2014).
176. Wang, Q. et al. Thermal and magnetic dual-responsive L-proline nano hybrids for aqueous asymmetric aldol reaction. *React. Funct. Polym.* **149**, 104508 (2020).
177. Tang, J. et al. Pickering interfacial catalysts with CO₂ and magnetic dual response for fast recovering in biphasic reaction. *ACS Appl. Mater. Interfaces* **11**, 16156–16163 (2019).
178. Anelli, P. L., Biffi, C., Montanari, F. & Quici, S. Fast and selective oxidation of primary alcohols to aldehydes or to carboxylic acids and of secondary alcohols to ketones mediated by oxoammonium salts under two-phase conditions. *J. Org. Chem.* **52**, 2559–2562 (1987).
179. Karami, B., Hoseini, S. J., Eskandari, K., Ghasemi, A. & Nasrabadi, H. Synthesis of xanthene derivatives by employing Fe₃O₄ nanoparticles as an effective and magnetically recoverable catalyst in water. *Catal. Sci. Technol.* **2**, 331–338 (2012).

180. Pagoti, S., Surana, S., Chauhan, A., Parasar, B. & Dash, J. Reduction of organic azides to amines using reusable Fe₃O₄ nanoparticles in aqueous medium. *Catal. Sci. Technol.* **3**, 584–588 (2013).
181. Piermattei, A., Karthikeyan, S. & Sijbesma, R. Activating catalysts with mechanical force. *Nat. Chem.* **1**, 133–137 (2009).
182. Groote, R., Jakobs, R. T. M. & Sijbesma, R. P. Mechano catalysis: forcing latent catalysts into action. *Polym. Chem.* **4**, 4846–4859 (2013).
183. Pickhardt, W., Grätz, S. & Borchardt, L. Direct mechanocatalysis: using milling balls as catalysts. *Chem. Eur. J.* **26**, 12903–12911 (2020).
184. Schumacher, C. et al. Mechanochemical dehydrocoupling of dimethylamine borane and hydrogenation reactions using Wilkinson's catalyst. *Chem. Commun.* **54**, 8355–8358 (2018).
185. Maity, C. & Das, N. Alginate-based smart materials and their application: recent advances and perspectives. *Top. Curr. Chem. (Z.)* **380**, 3 (2022).
186. Robertson, J. C., Coote, M. L. & Bissemer, A. C. Synthetic applications of light, electricity, mechanical force and flow. *Nat. Rev. Chem.* **3**, 290–304 (2019).

Acknowledgements

Author (C.M.) acknowledges the funding from the Science and Engineering Research Board (SERB)-Department of Science and Technology (DST) as Start-up research grant (No. – SRG/2020/000571). N.D. thanks DST for INSPIRE fellowship (Ref. No. – DST/INSPIRE/03/2022/000179). Authors (C.M. and N.D.) thank the management of VIT, Vellore for the support.

Author contributions

C.M. conceived the scope of the article. N.D. and C.M. searched the literature, constructed the topics, and wrote the manuscript. C.M. supervised the work. All authors revised and commented on the manuscript.

Competing interests

The authors declare no competing interests.

Additional information

Correspondence and requests for materials should be addressed to Chandan Maity.

Peer review information *Communications Chemistry* thanks Robert Göstl and the other, anonymous, reviewer(s) for their contribution to the peer review of this work.

Reprints and permission information is available at <http://www.nature.com/reprints>

Publisher's note Springer Nature remains neutral with regard to jurisdictional claims in published maps and institutional affiliations.



Open Access This article is licensed under a Creative Commons Attribution 4.0 International License, which permits use, sharing, adaptation, distribution and reproduction in any medium or format, as long as you give appropriate credit to the original author(s) and the source, provide a link to the Creative Commons license, and indicate if changes were made. The images or other third party material in this article are included in the article's Creative Commons license, unless indicated otherwise in a credit line to the material. If material is not included in the article's Creative Commons license and your intended use is not permitted by statutory regulation or exceeds the permitted use, you will need to obtain permission directly from the copyright holder. To view a copy of this license, visit <http://creativecommons.org/licenses/by/4.0/>.

© The Author(s) 2022